

united nations
educational, scientific
and cultural
organization



international atomic
energy agency

the

abdus salam

international centre for theoretical physics

ICTP/UCSB/TWAS

MINIWORKSHOP ON "FRONTIERS IN MATERIALS SCIENCE"

15 - 18 May 2001

301/1311-3

*"Structural & Chemical Analysis of Materials by Advanced
Transmission Electron Microscopy Technique"*

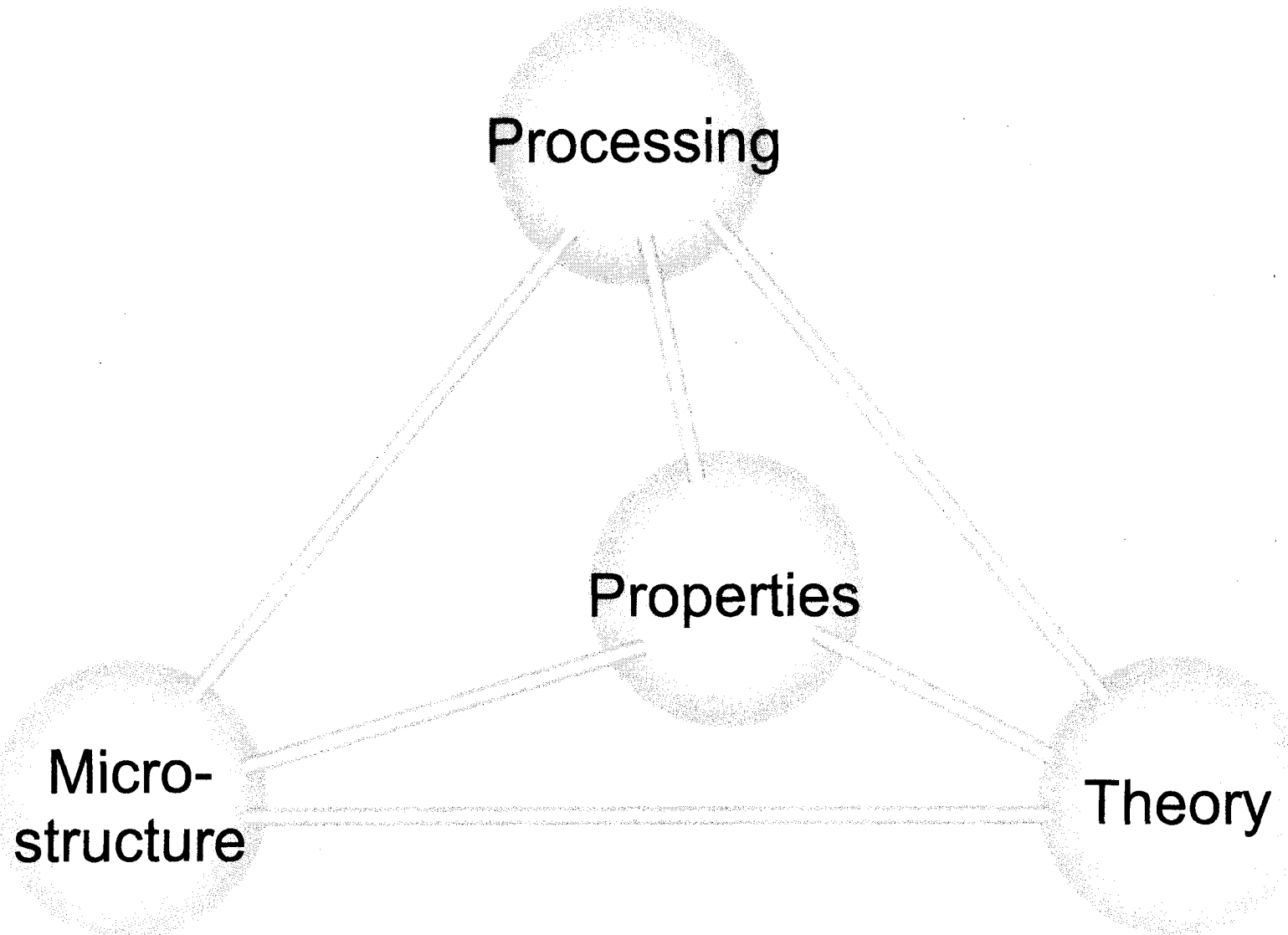
M. RÜHLE
Max-Planck-Institut für Metallforschung
Stuttgart
Germany

Please note: These are preliminary notes intended for internal distribution only.

Structural and Chemical Analysis of Materials by Advanced Transmission Electron Microscopy Technique

Manfred Rühle
Max-Planck-Institut für Metallforschung
Seestr. 92, 70714 Stuttgart, Germany

Materials Science



Outline

Introduction: Pathways of microstructural analysis
bridging length scales over many dimensions

Transmission Electron Microscopy:
Different Techniques
Advantages and Problems

Case Studies

Defects in Metals (Cu, NiAl, ...)

Defects in Ceramics (Al_2O_3 , SrTiO_3 , ...)

Defect at Metal/Ceramic Composites

Nature of Defects

0-dimensional: point defects, point defect cluster

1-dimensional: dislocation

2-dimensional: interfaces

3-dimensional: inclusions

Acknowledgement

K. van Benthem, S. Krämer, C. Scheu, W. Sigle

Specimen preparation: W. Kurtz, T. Wagner

TEM specimen preparation: U. Salzberger, A. Strecker, M. Sycha

Financial Support

DFG (German Science Foundation)

Volkswagen Foundation

State of Baden-Württemberg

Max Planck Society

Microstructural Parameters

Phases present in materials

Grain sizes

Grain size distribution

Grain shape

Misorientation of grains ("special" boundaries)

Composition of regions close to the GB

Atomic structure of specific GBs

Bonding

X-ray techniques, microprobe

OM, quantitative analysis

SEM

OIM, SAD (in TEM)

Q-AEM

Q-HREM

ELNES: fingerprints and
quantitative analysis

Microscopy of Materials:

Many lenght scales!

Optical Microscopy

Conventional Optical Microscopy
Laser-Scanning Microscopy
Near Field Optical Microscopy
Video Microscopy

Electron Microscopy

Scanning Electron Microscopy
Imaging
Chemical Analysis

Transmission Electron Microscopy

Diffraction Studies
Diffraction Contrast
Atomic-Resolution Microscopy
Analytical Studies
Energy Dispersive Studies
Electron Energy Loss Spectroscopy
Electron Loss Near Edge Structure

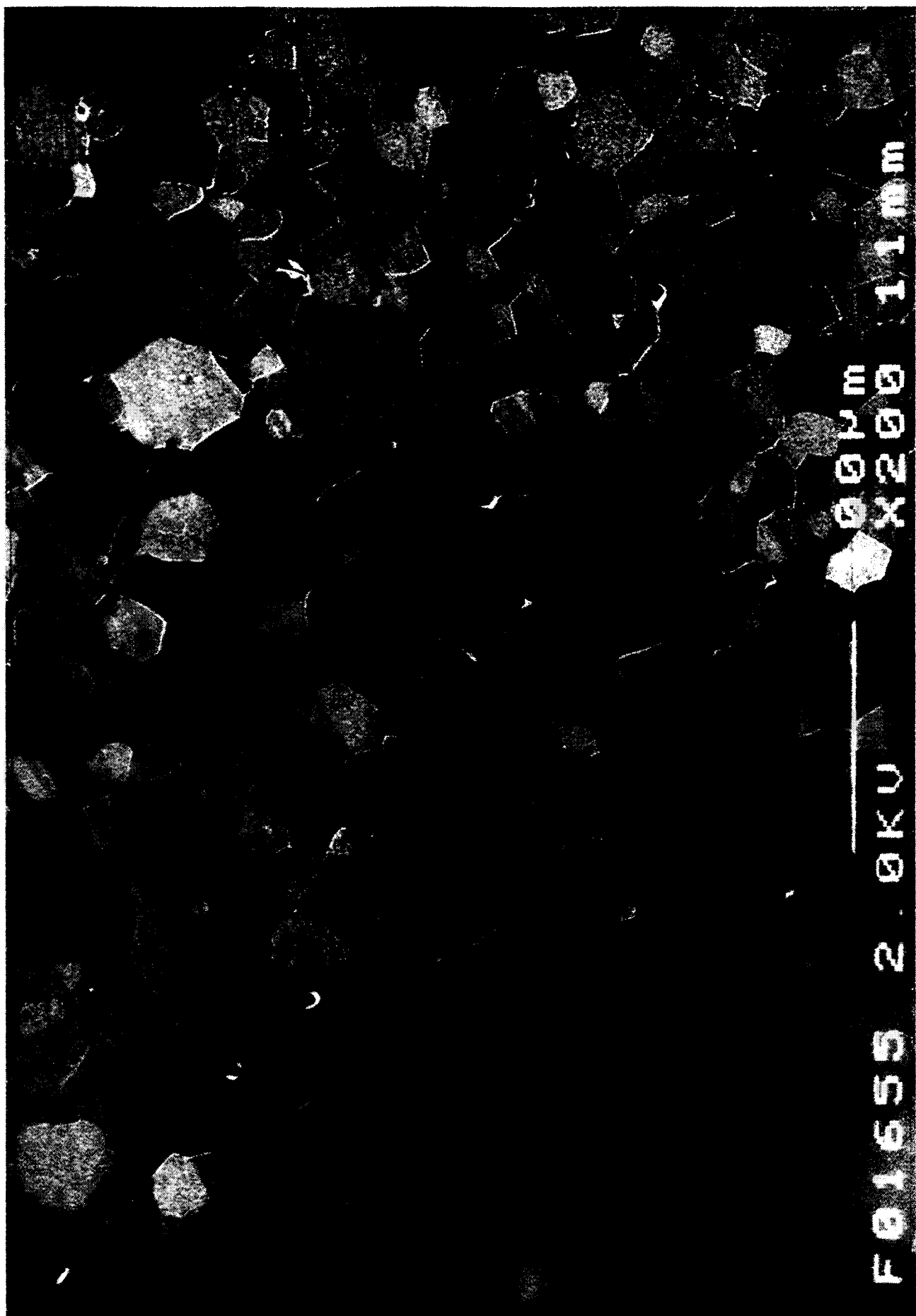
Atom Probe Field-Ion Microscopy

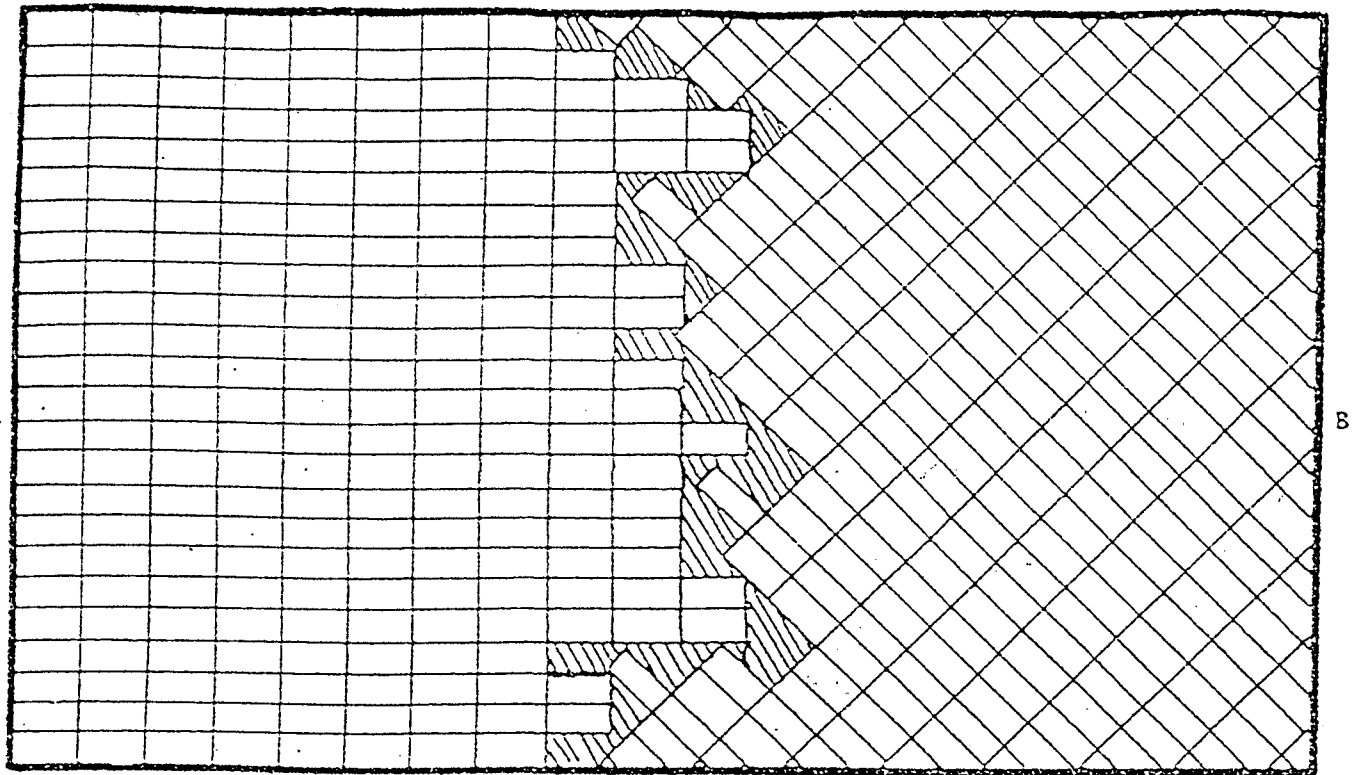
Probe Techniques:
Scanning Tunneling Microscopy (STM)
Scanning Tunneling Spectroscopy
Atomic Force Microscopy (AFM)

11 mm

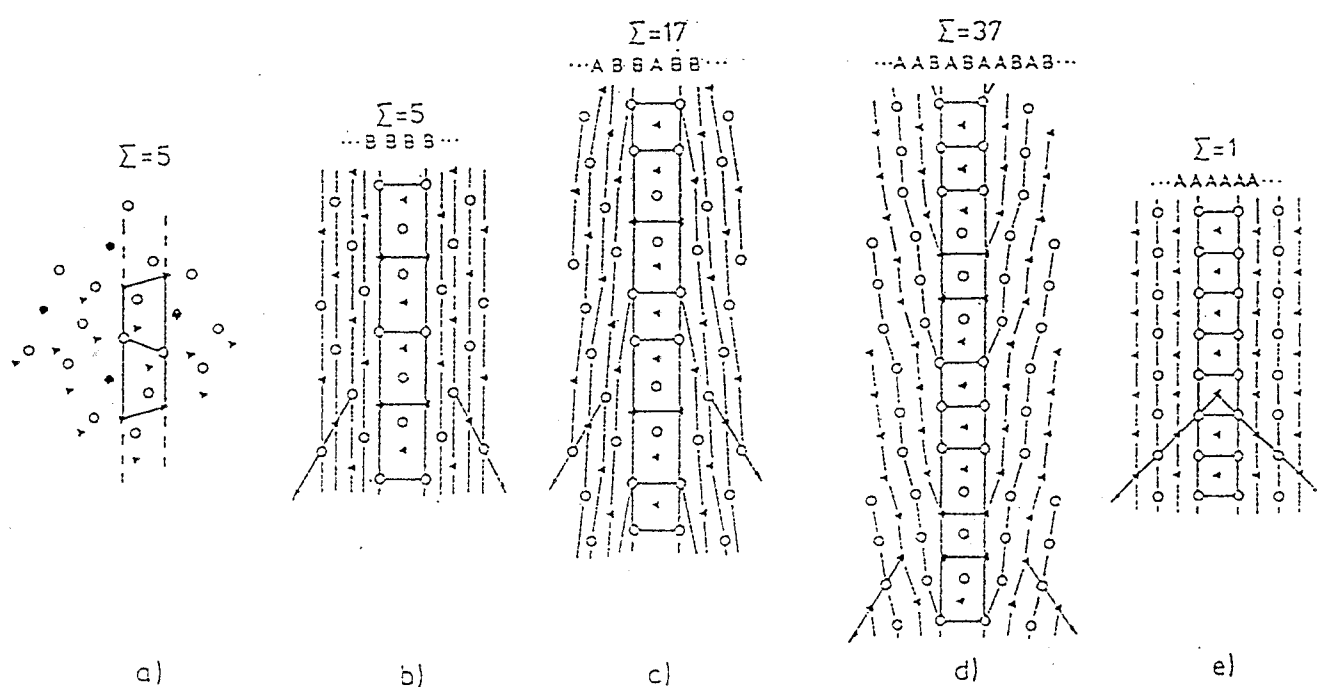
mm
100
90
80

F 01555 2 . 9 KU

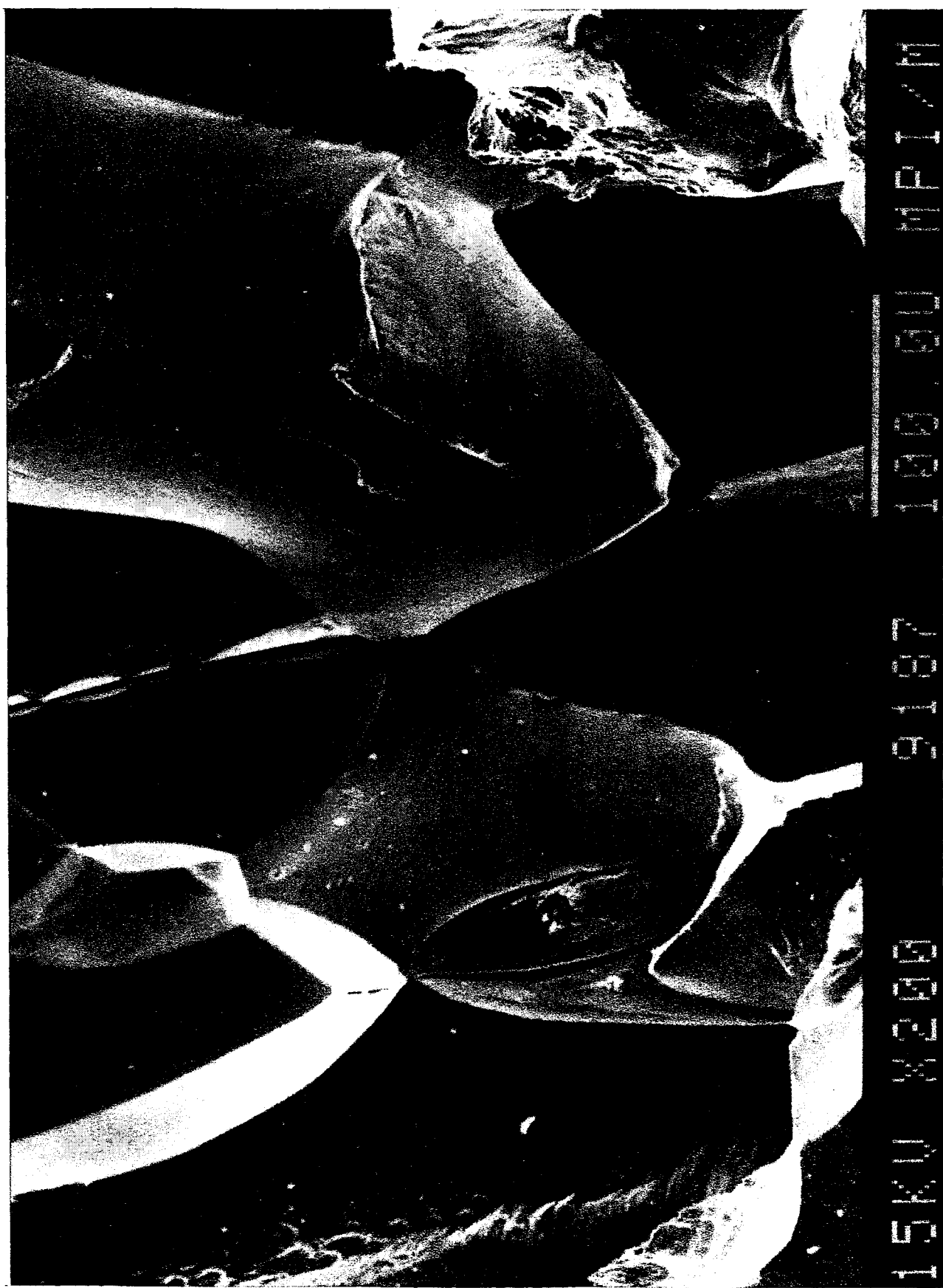


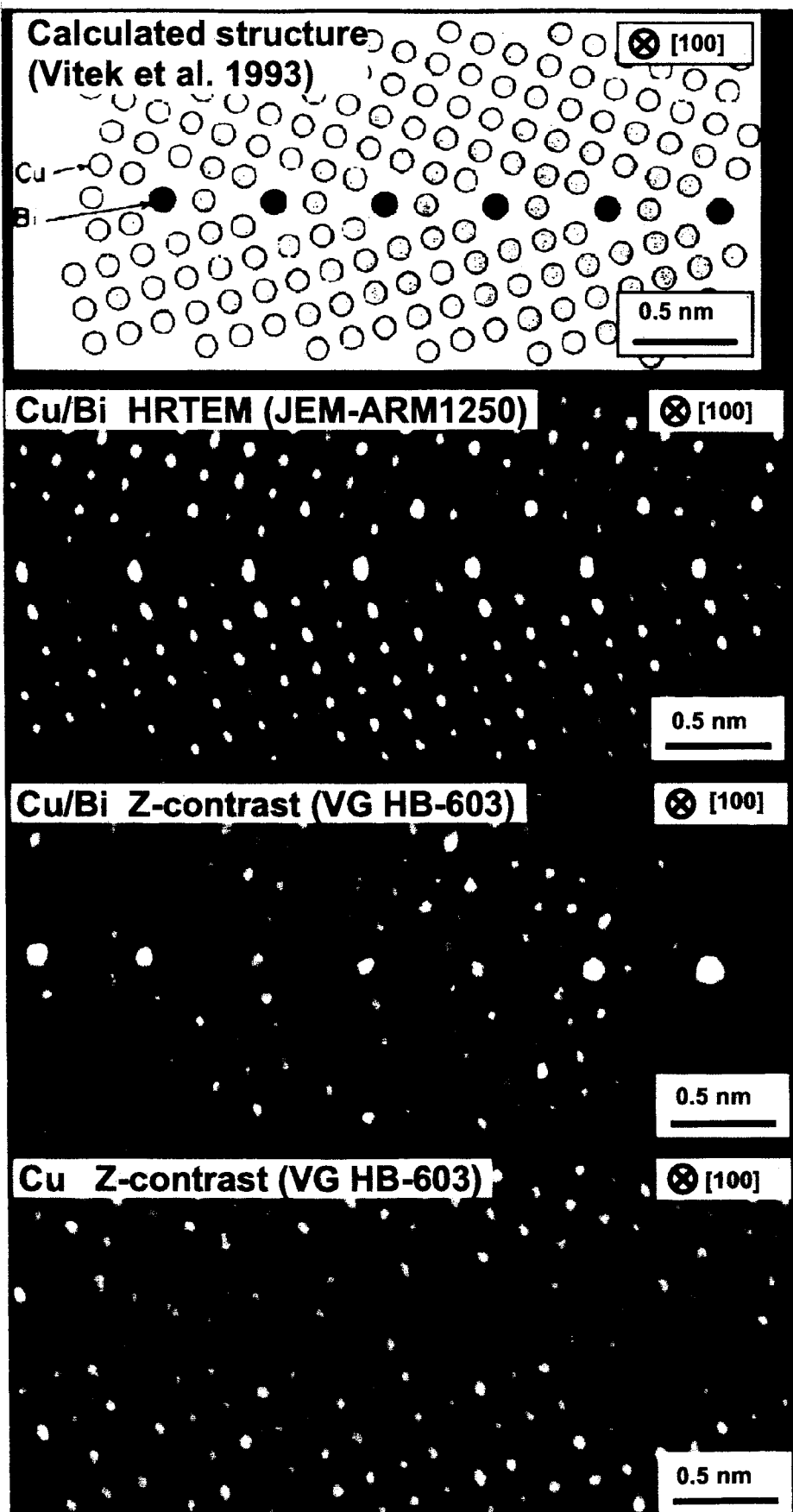


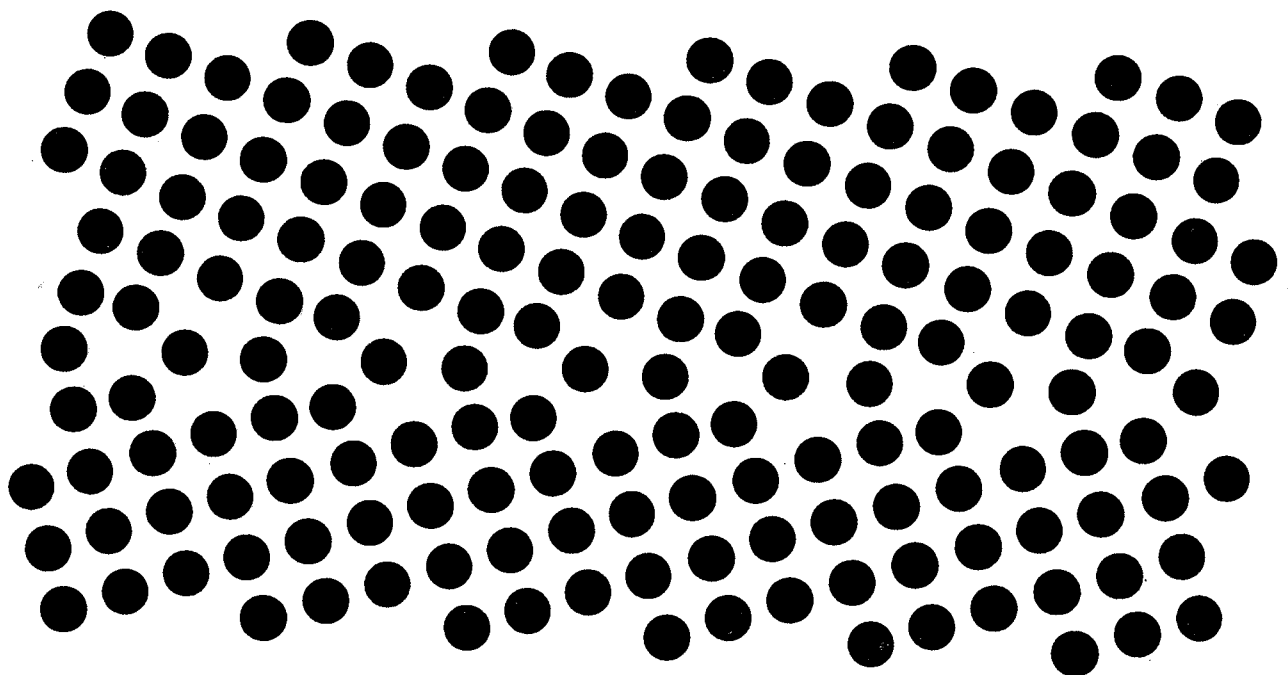
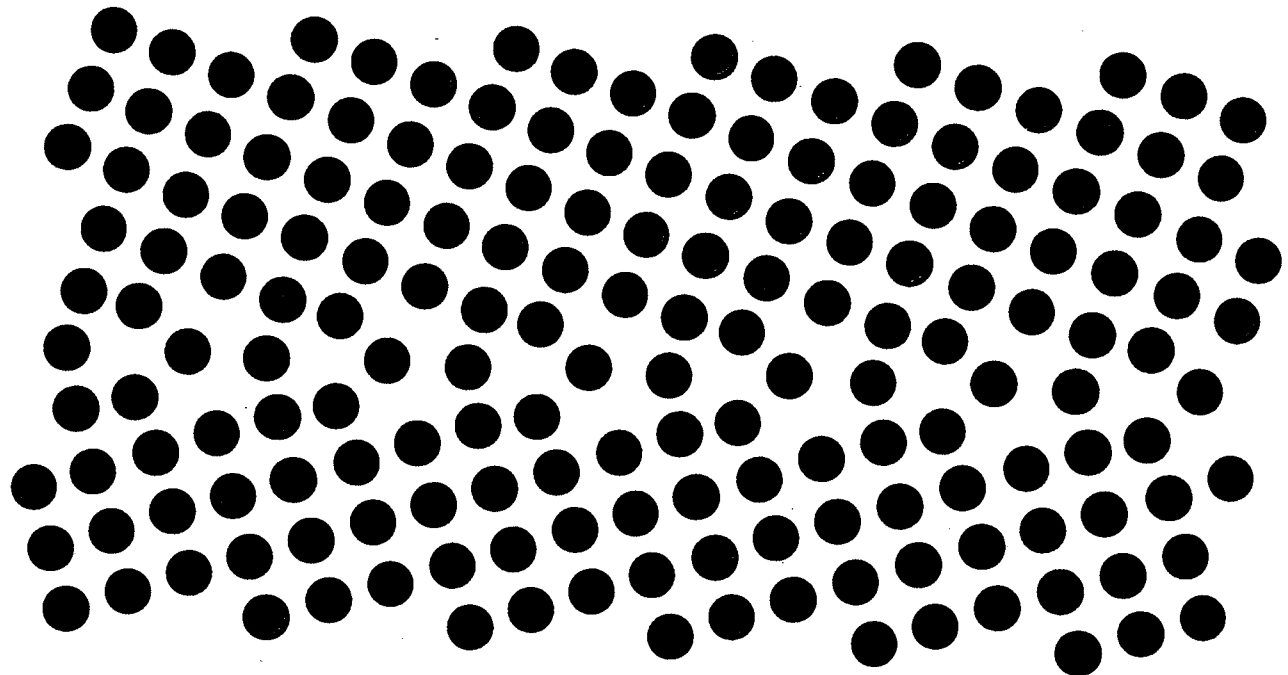
Rosenhain, Ewen. 1912



Sutton, Vitek 1983







Transmission Electron Microscopy

Conventional TEM

BF/DF/SAD

- Morphology
- Phase Distribution
- Defect Analysis
- *in situ*-Experiments
 - heating
 - cooling
 - deformation

Spectroscopy and CBED

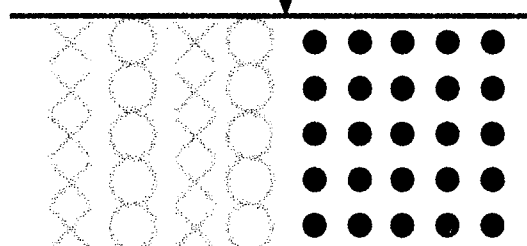
(high spatial resolution)

- EDS
 - compositions
 - gradients
- EELS (EXELFS, ELNES)
 - compositions
 - gradients
 - electronic states

Lattice Imaging

HREM

- Structure of materials
 - oxides
 - HT superconductors
- Structure of defects
 - interfaces
 - dislocations



Information on chemistry and bonding

Complicated evaluation:
lens aberration of HREM
scattering within specimen

Experimental studies

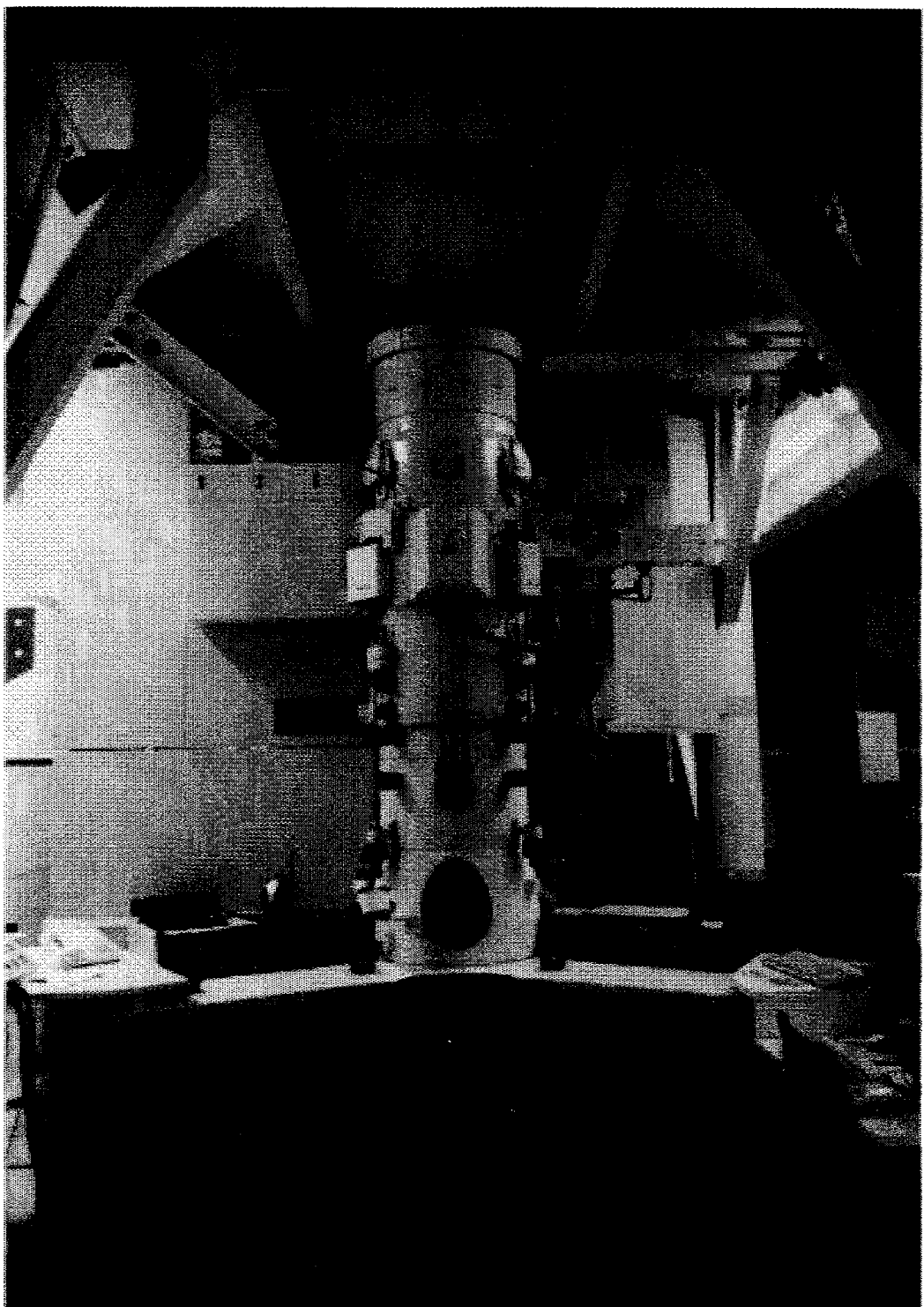


Image simulations

point-to-point 1.0 Å }
information limit 0.8 Å } 1250 kV

STUTTGART
"ATOMIC RESOLUTION MICROSCOPE"

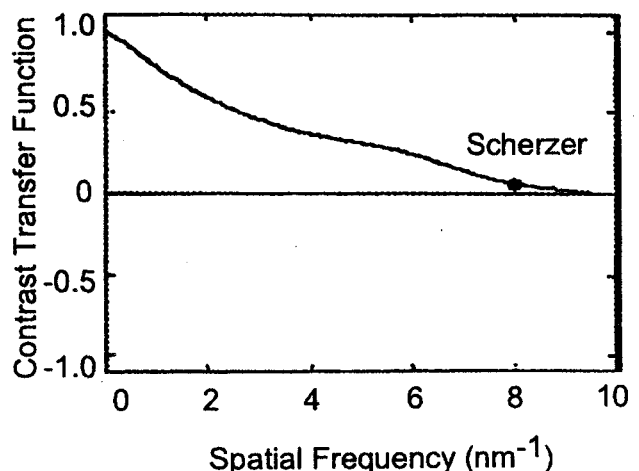
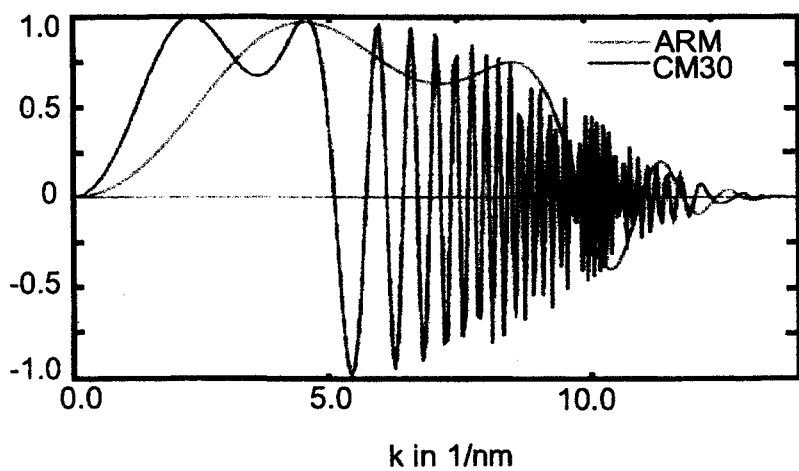
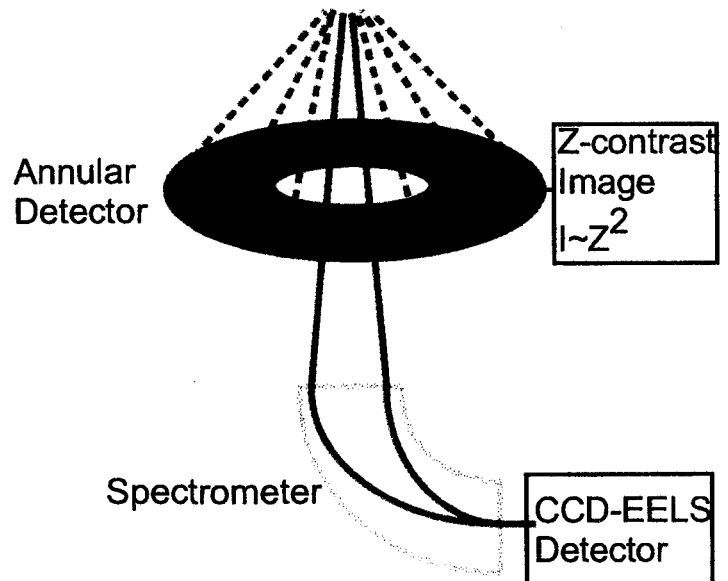
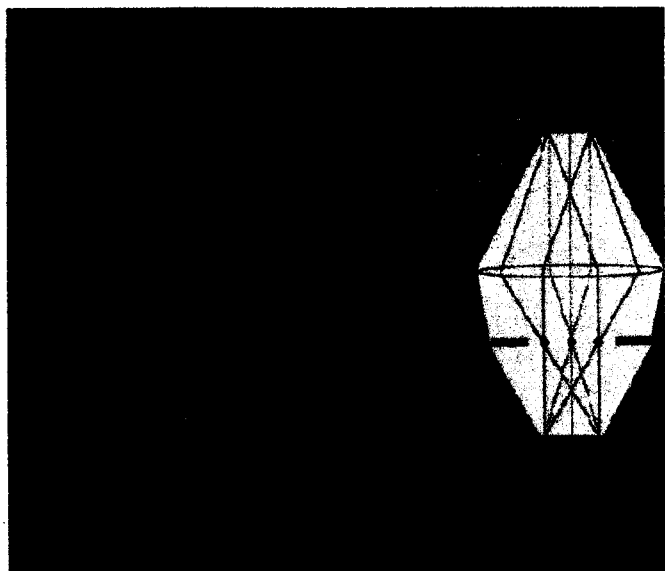
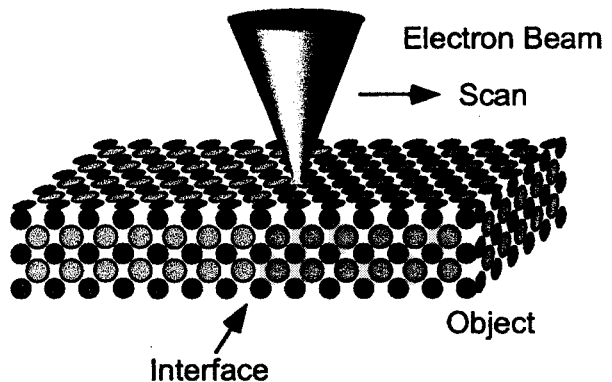
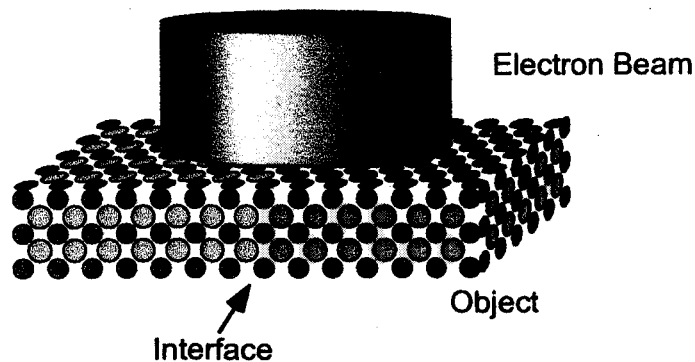
JEM-ARM1250



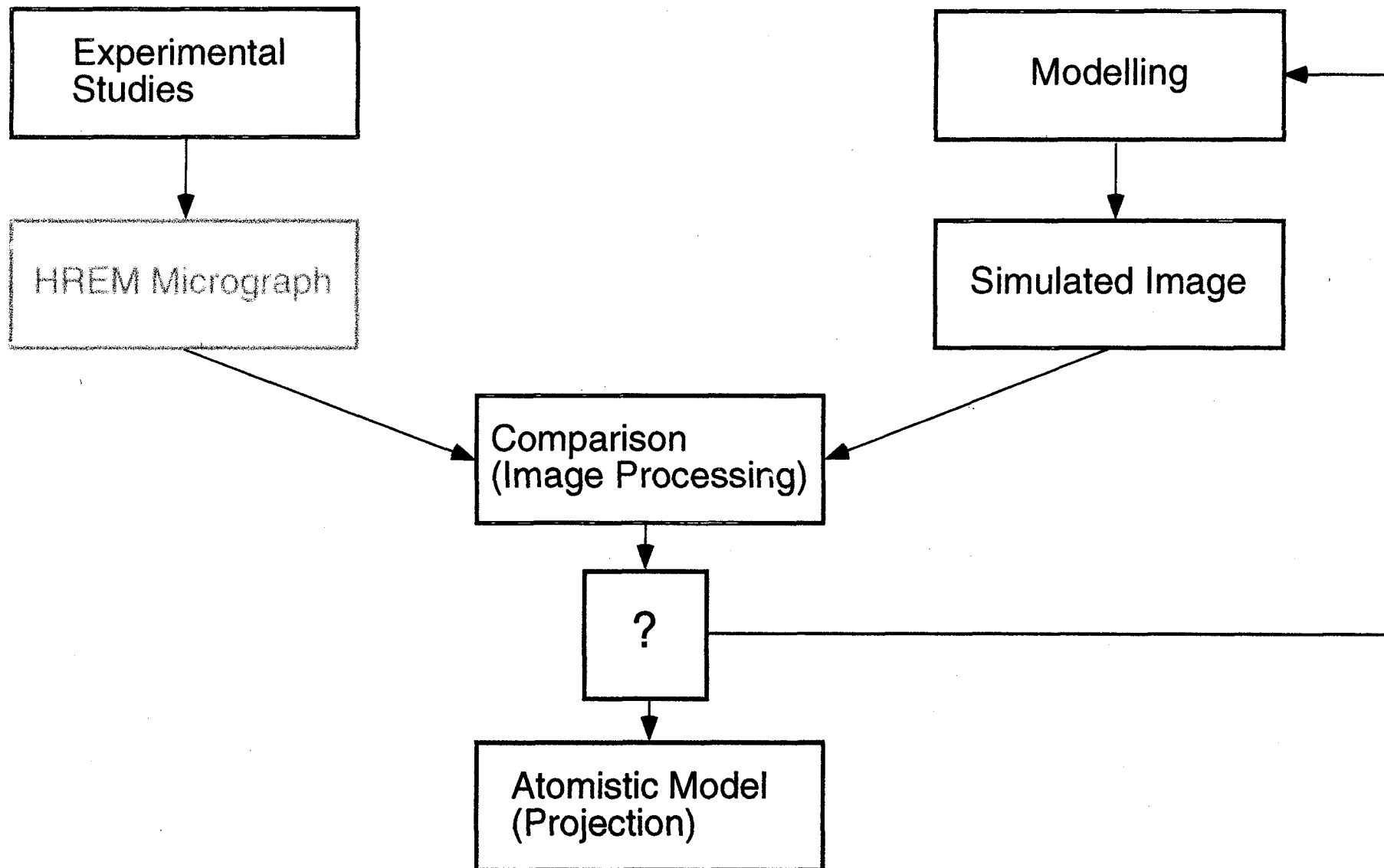
High-Resolution Transmission Electron Microscopy

coherent imaging

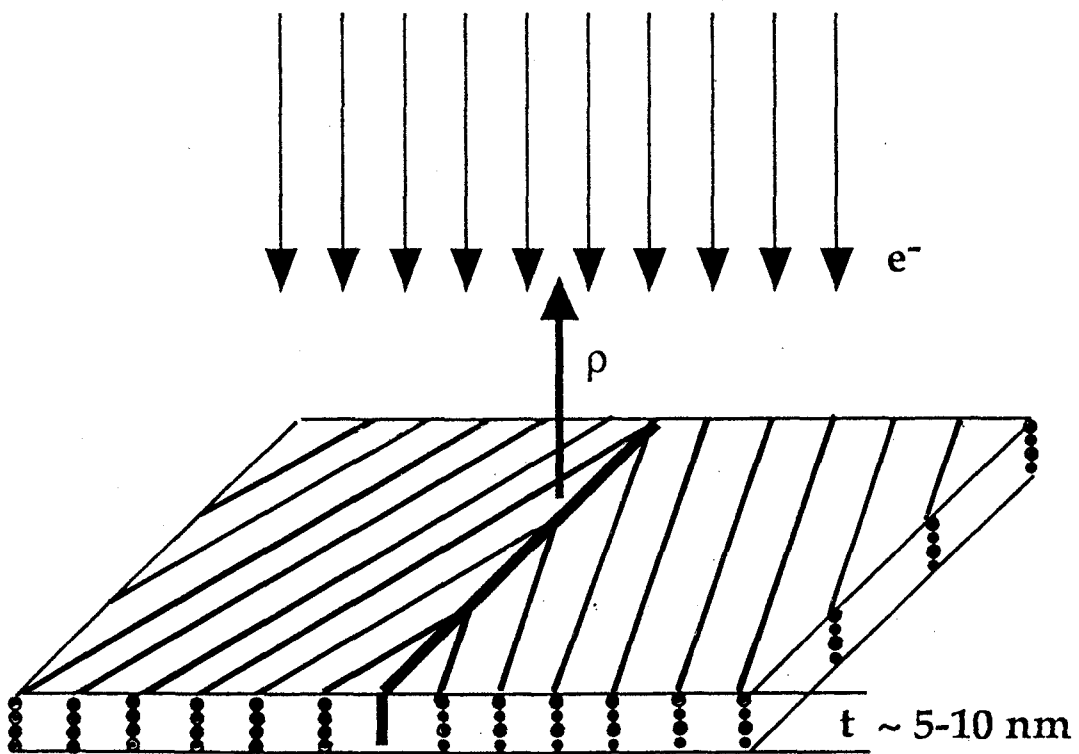
incoherent imaging
(Z-contrast)



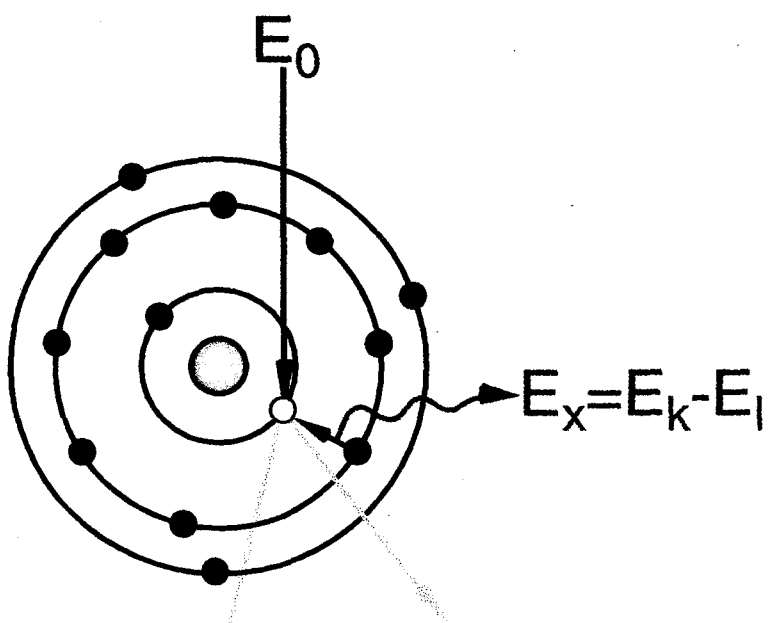
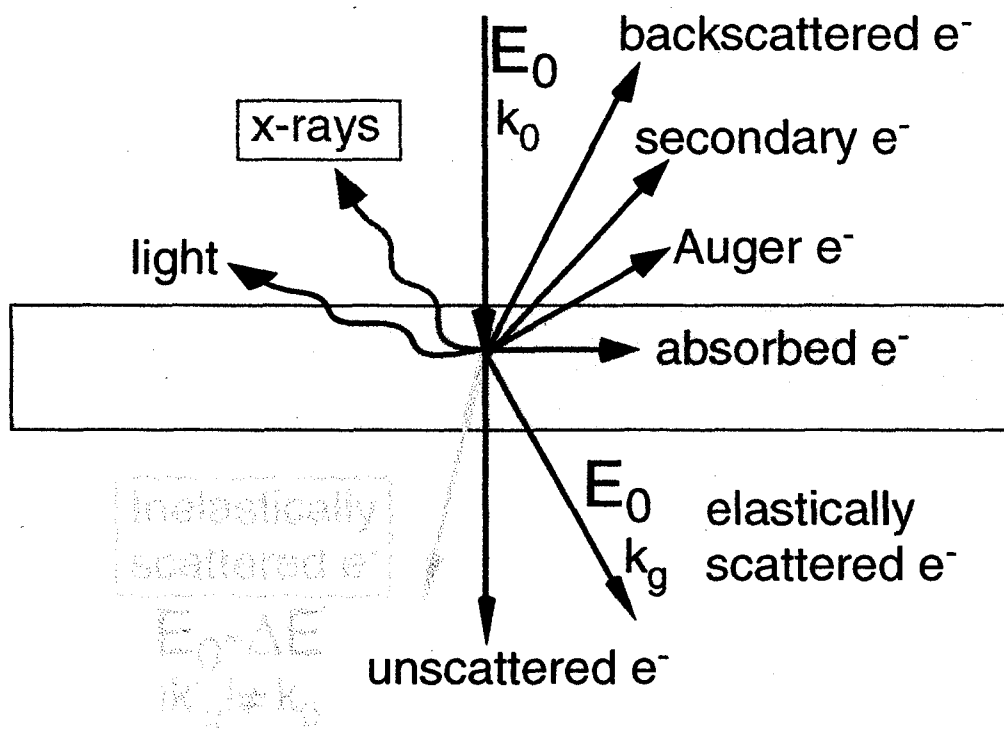
Quantitative High-Resolution Electron Microscopy



High Resolution Electron Microscopy of Interfaces



Elastic and Inelastic Scattering Process



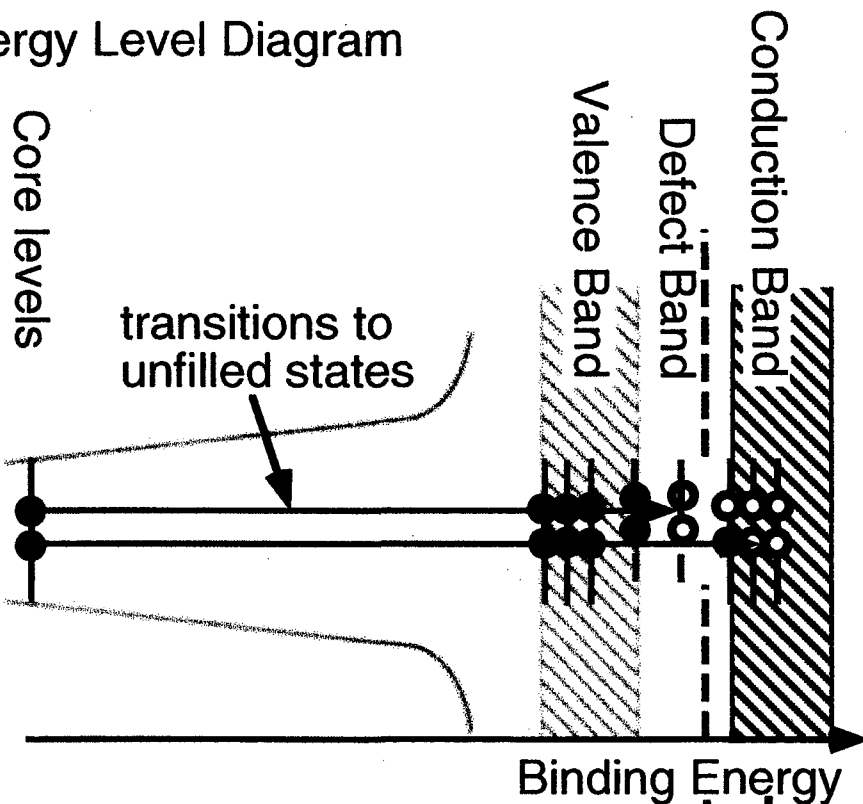
EDS
Energy Dispersive
Spectroscopy

EDS
Energy Dispersive
Spectroscopy

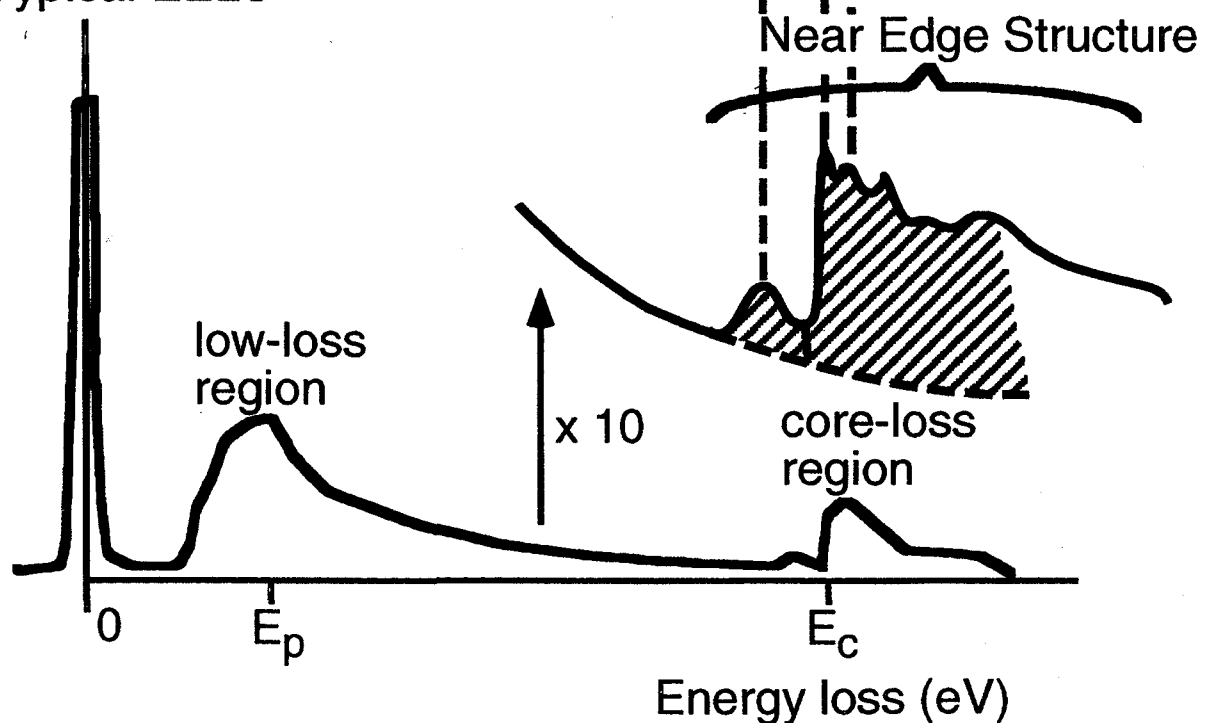
ELNES

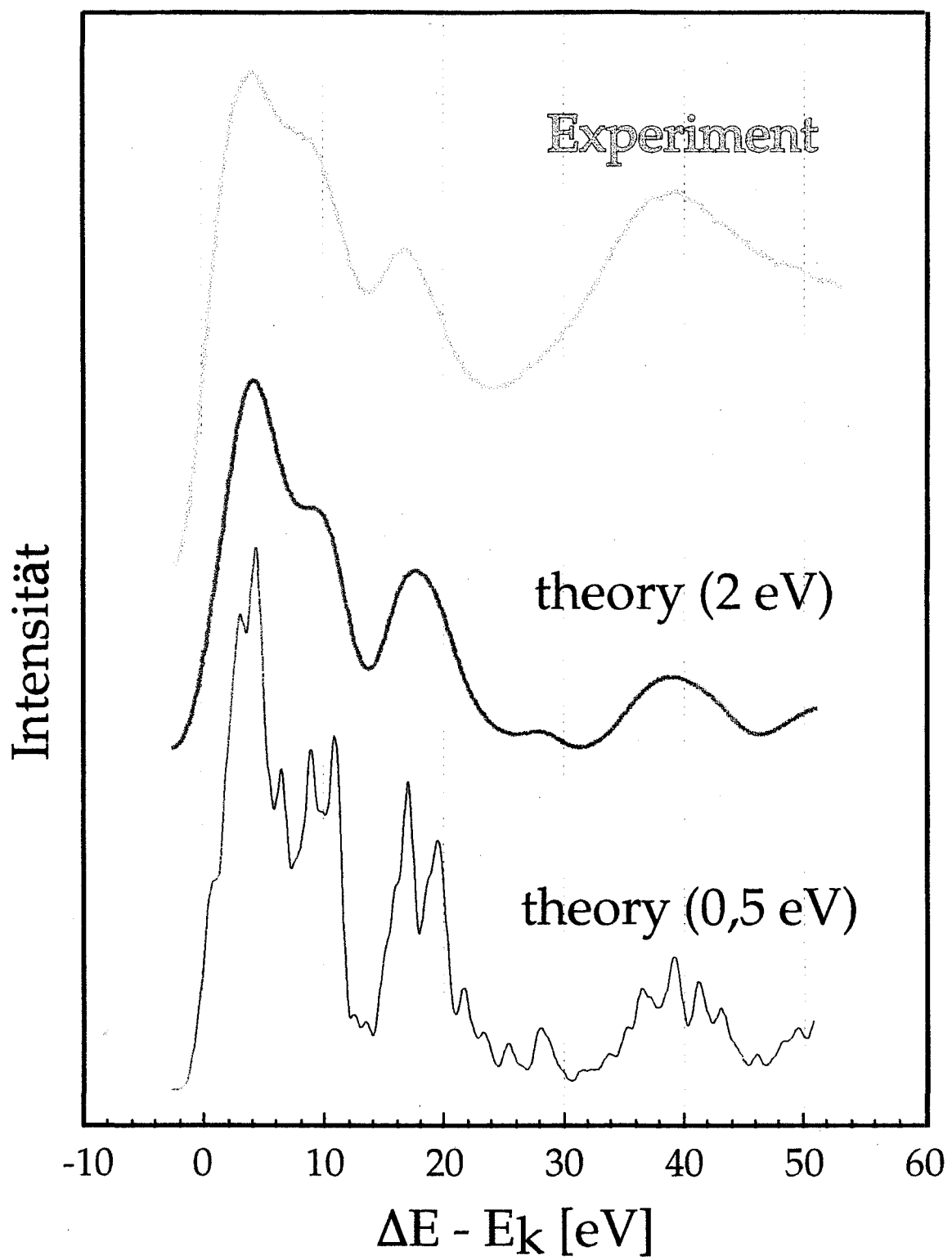
(electron energy-loss near edge structure)

Energy Level Diagram

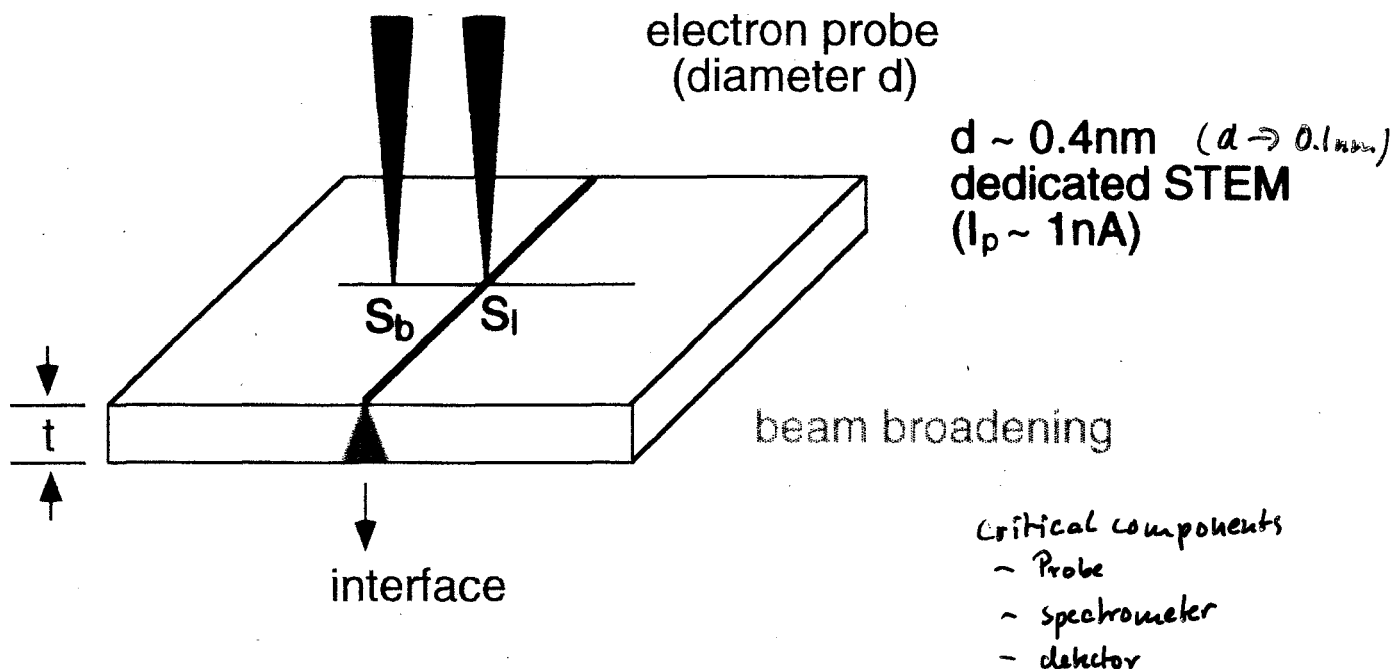


Typical EELS





Analytical Electron Microscopy with High Spatial Resolution



Comparision of S_b and S_l : (EDS and EELS)

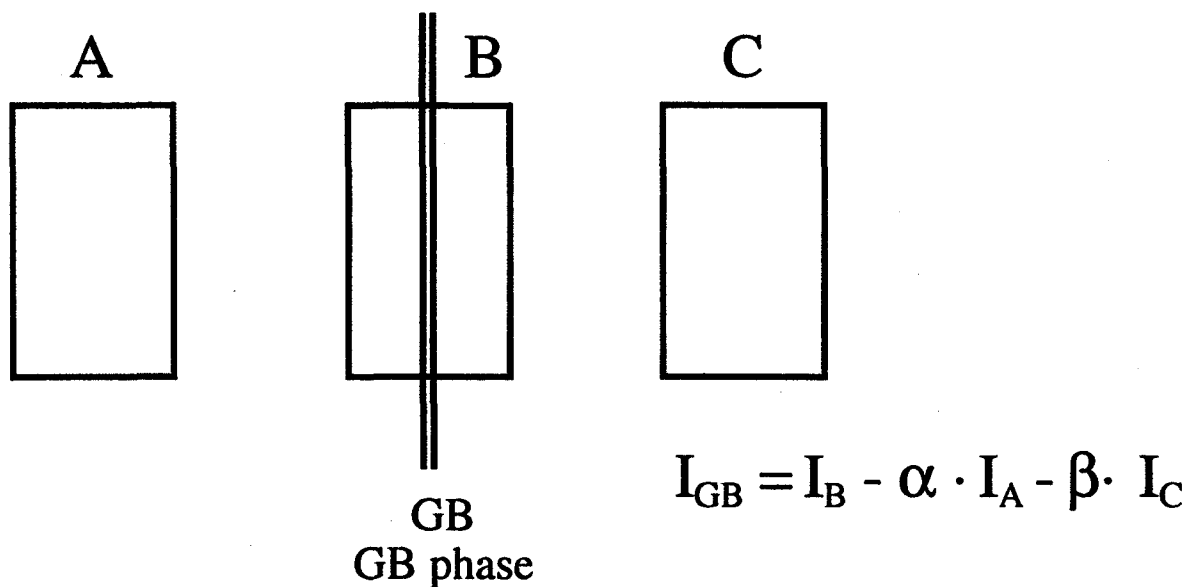
- Segregation
- ELNES -> information on local bandstructures
SREELS : Spacially Resolved

Special techniques (with dedicated instruments)

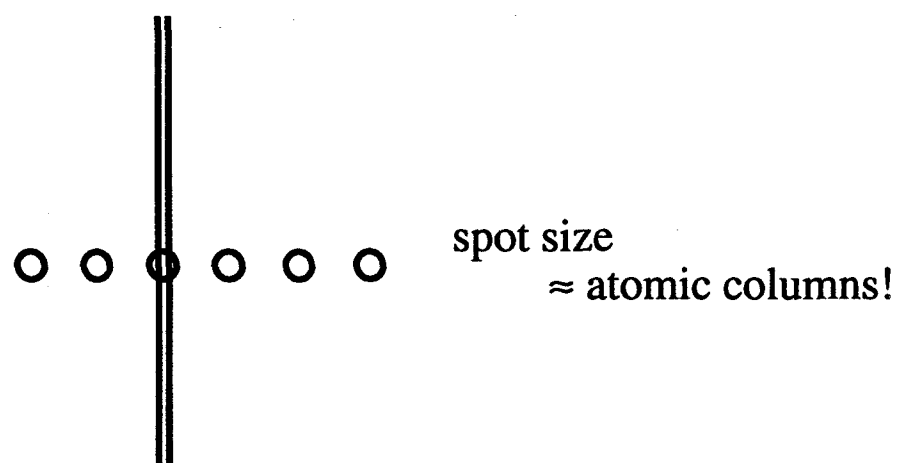
space charges at interfaces

EELS (ELNES) of Grain Boundaries

Spatial difference technique



spot mode



Spatial difference technique

- information on composition
- information on ELNES at interfaces

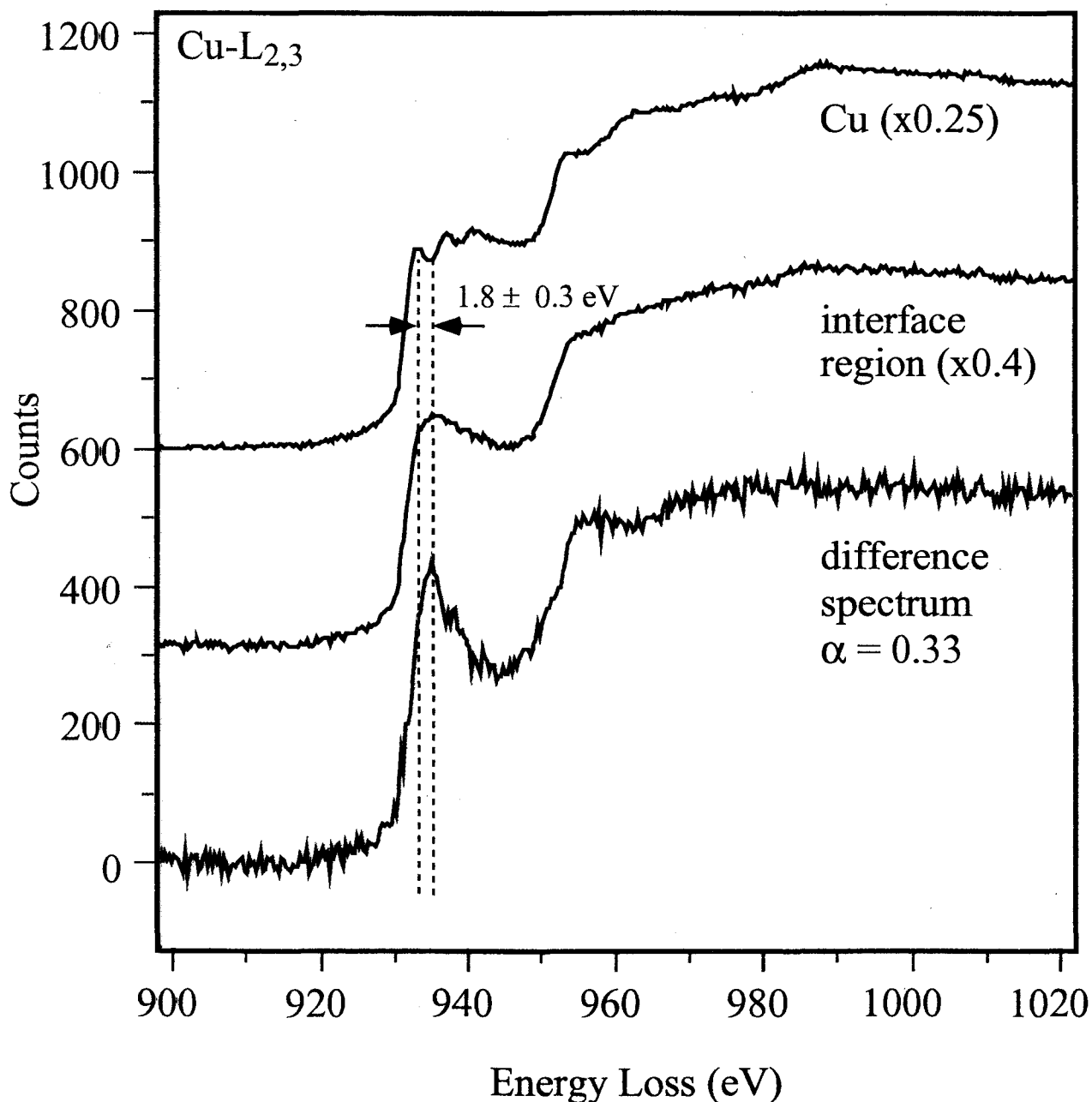
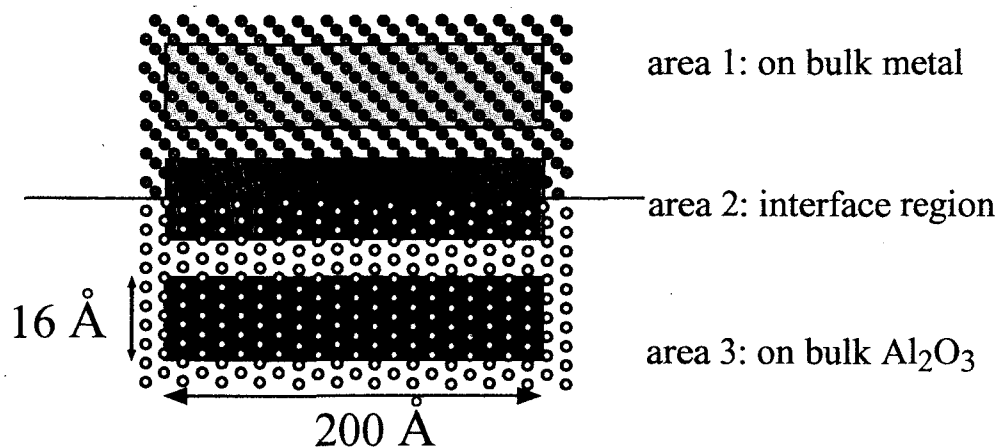
assumption: intensities of incoherent scattered electrons can be added

experimental "proof": C. Scheu

theoretical "proof": G. Möbus

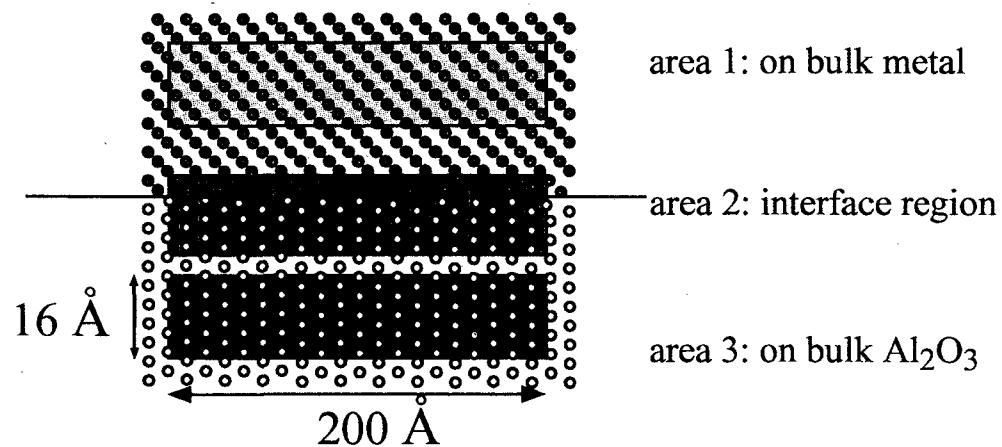
Results Cu/(0001)Al₂O₃ (MBE-Stuttgart T=600°C)

symmetrical case:



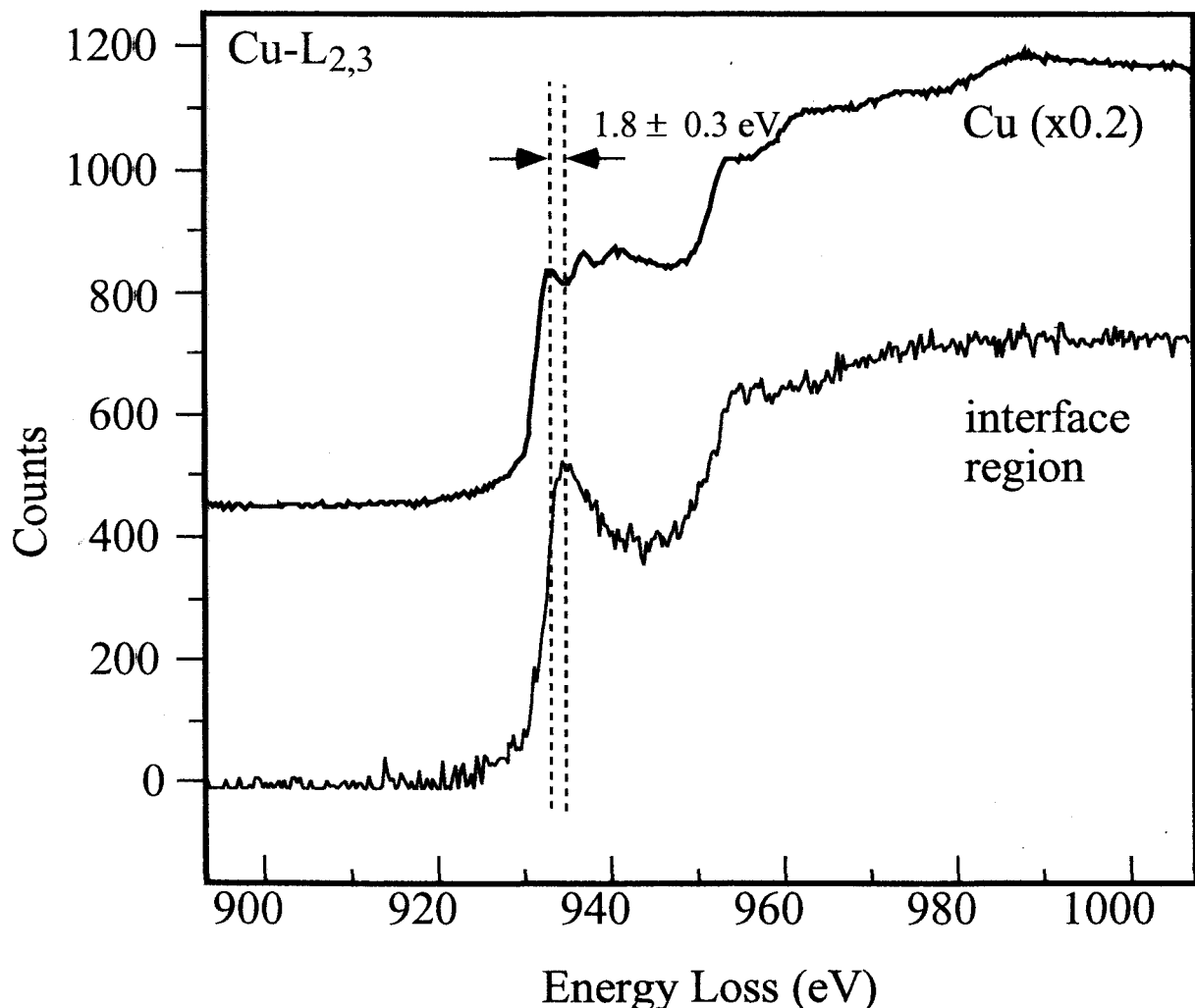
Cu/(0001)Al₂O₃ (T=600°C)

asymmetrical case:

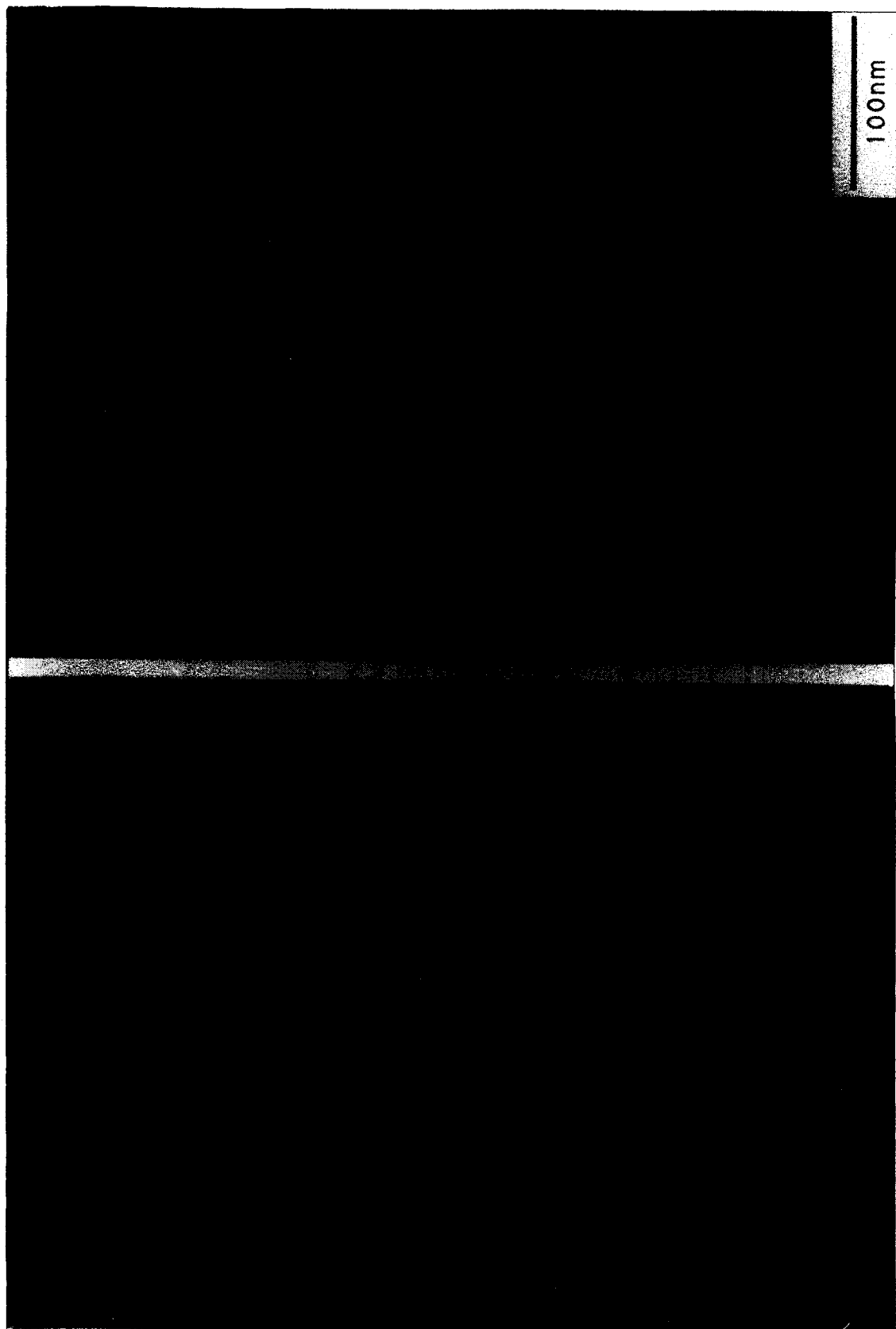


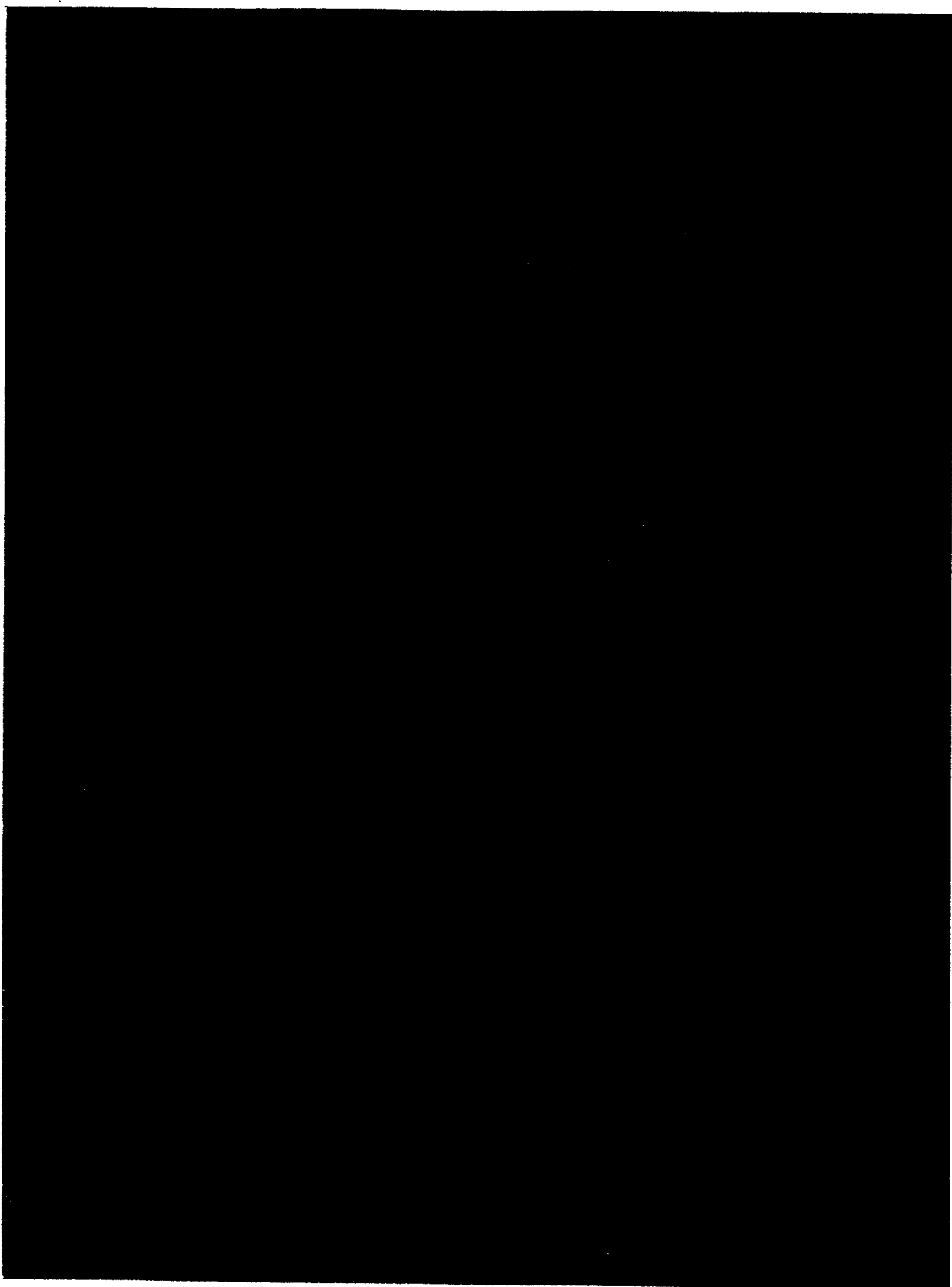
estimation of $\alpha = 0.08$

→ only 1.28 Å of the scanning area contains bulk Cu atoms!



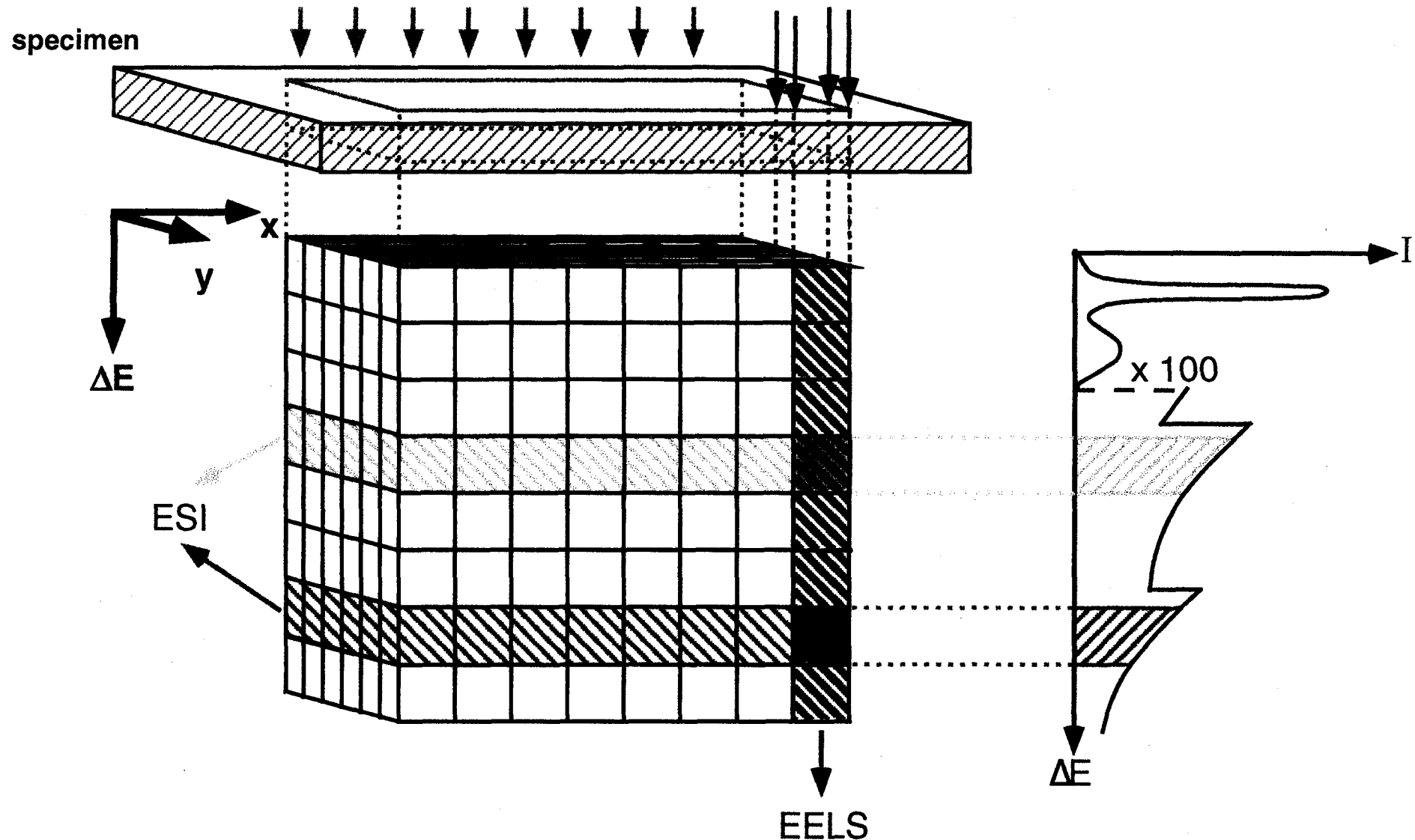
6/20



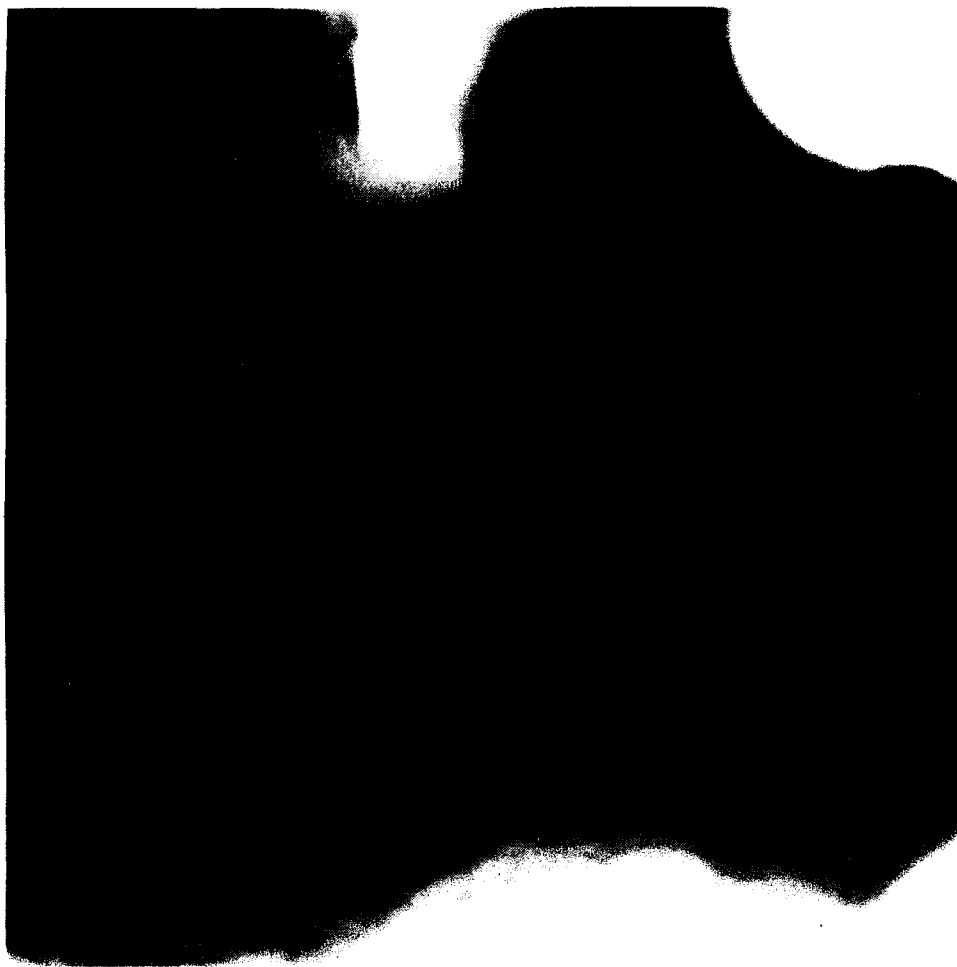


ESI

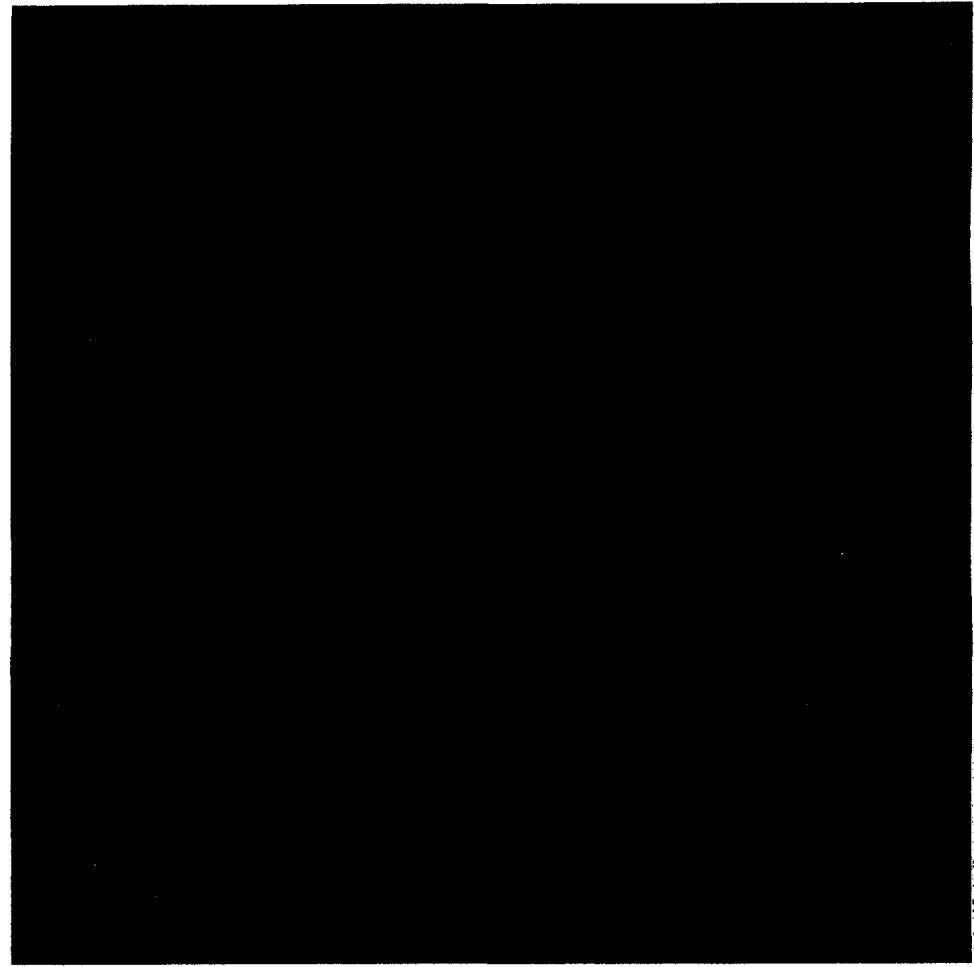
Image mode: $I = I(x, y, \Delta E)$



Sintered polymer derived $\text{Si}_3\text{N}_4/\text{SiC}$ -composite



(bright field image)



red: C (SiC)
green: N (Si_3N_4)
blue: O (am. oxide)

energy resolution
spatial resolution

Revolutionary Developments in Instrumentation

of TEM

- Spherical aberration (C_s) of magnetic lenses can be corrected! (Haider, Rose, Urban)
- Monochromators for electron source will soon be available (Rose)
- Energy filter for electrons with high transmittivity are available (Mandoline filter)
- Advanced detection systems allow collection of each electron (low noise CCD cameras)

FEG (200 kV)

Monochromator

Energy selecting
slit ($\Delta E \lesssim 0.2$ eV)

XEDS



Object

Objective
Lens

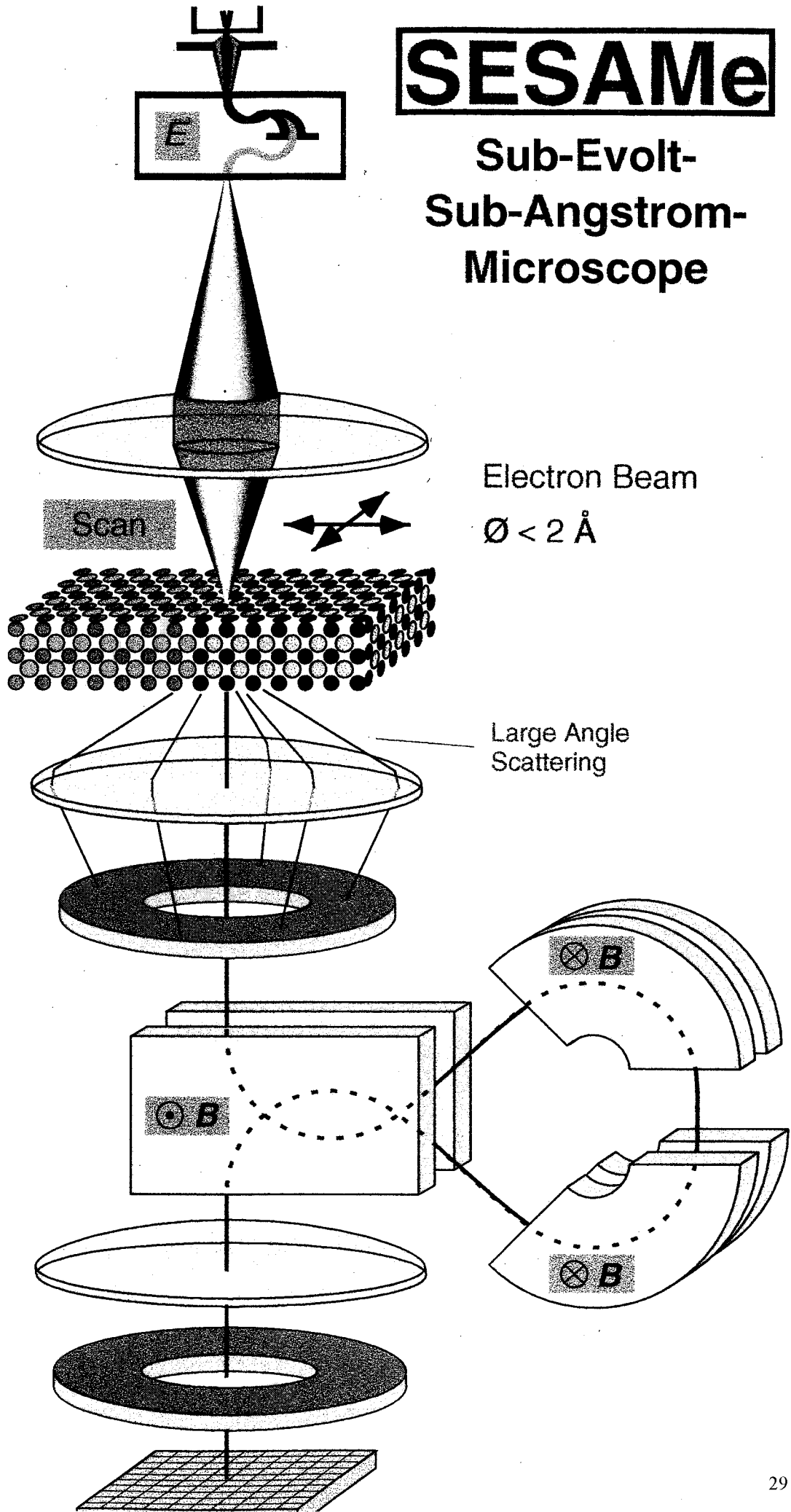
Annular Detector
»Z-Contrast«

Energy Filter
»Mandoline«

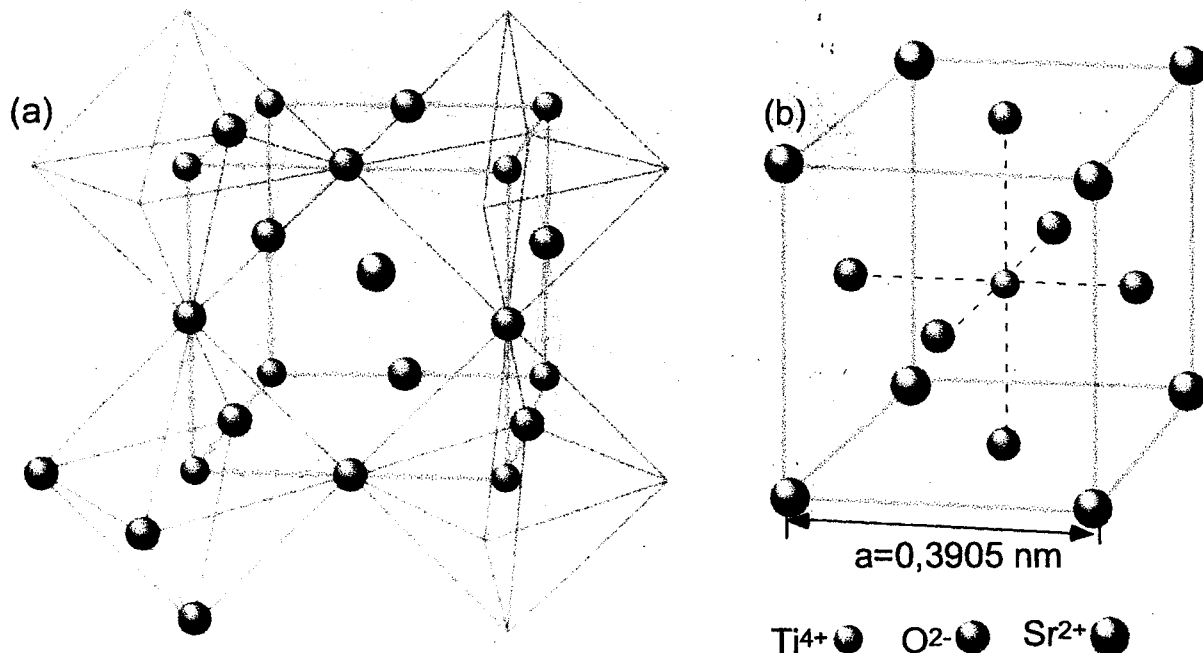
Projector
Lens

Energy filtered
Annular Detector

CCD



SrTiO₃ - Crystal Properties



Crystal structure of SrTiO₃. Titan is in 6-fold coordination by Oxygen.

Selected properties of SrTiO₃

Crystal structure : Perowskite
cubic → highly symmetrical complex structure

Lattice constant : $a = 0.3905 \text{ nm}$

Space group : Pm $\bar{3}m$

Moos hardness : 6...6.5

Single crystal orientation : (001) and (110)

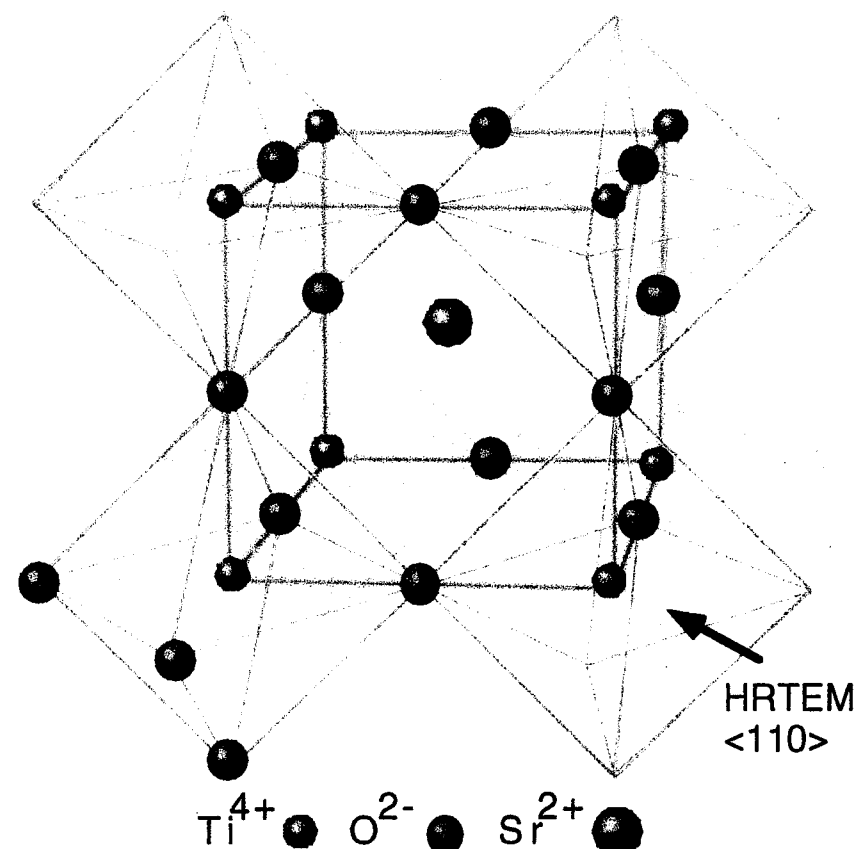
scattering factors?
charge density distribution?

crystallography

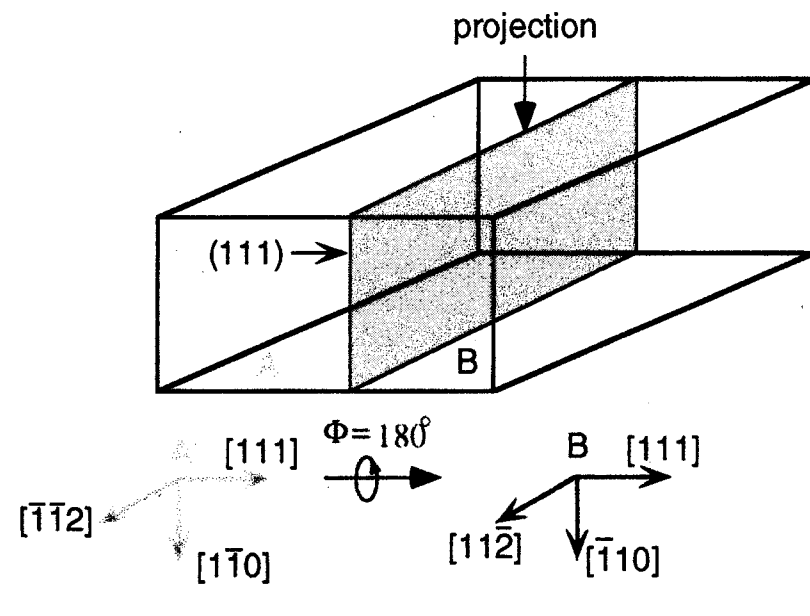
crystal structure of SrTiO_3

Perovskite

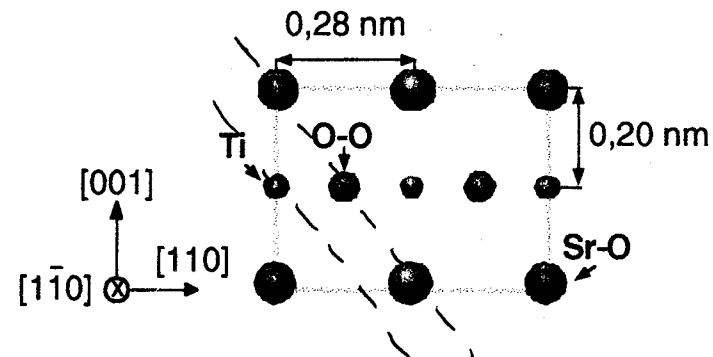
$\overline{\text{Pm}3\text{m}}$; $a = 0,3905 \text{ nm}$



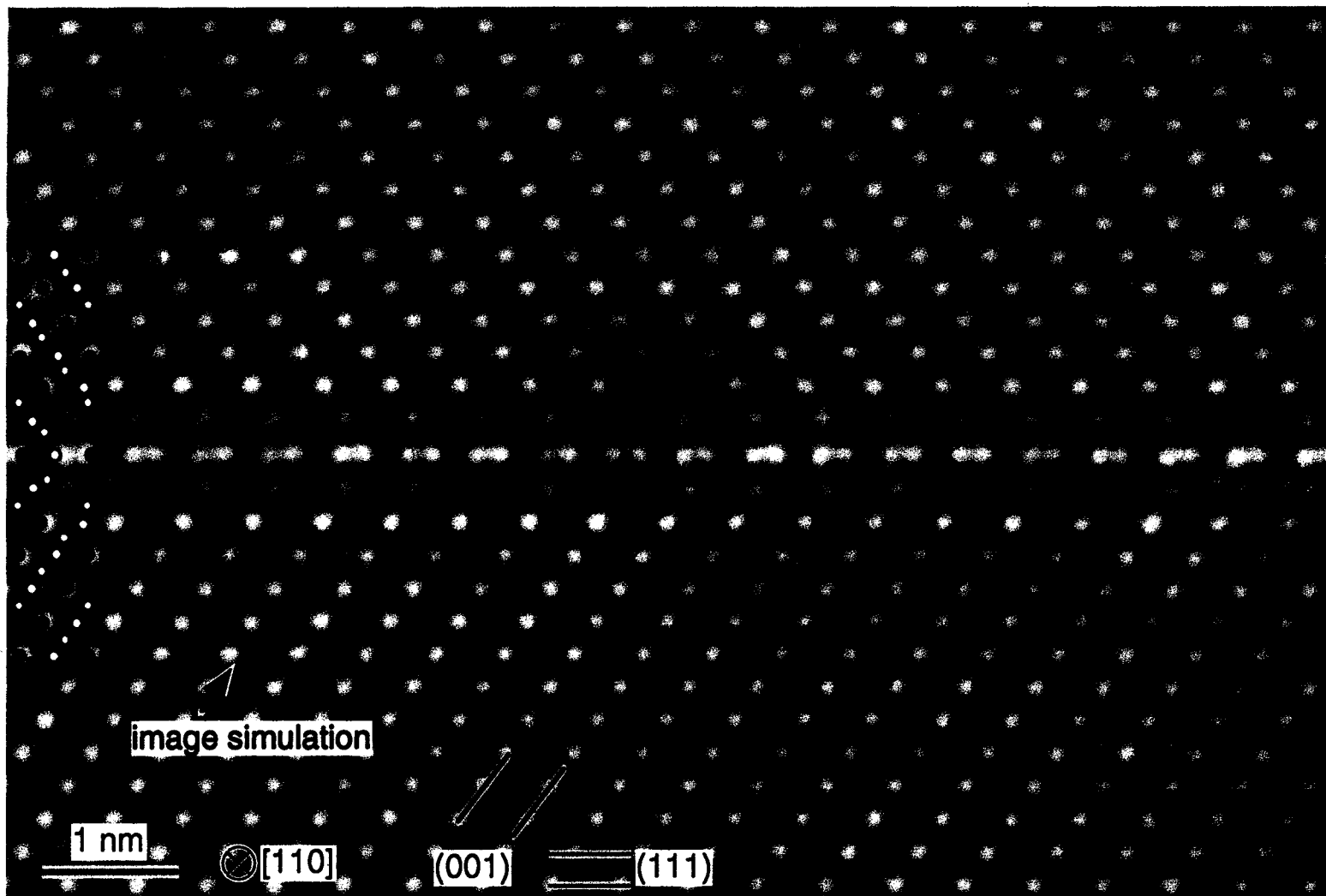
grain boundary crystallography



unit cell in $<110>$ projection

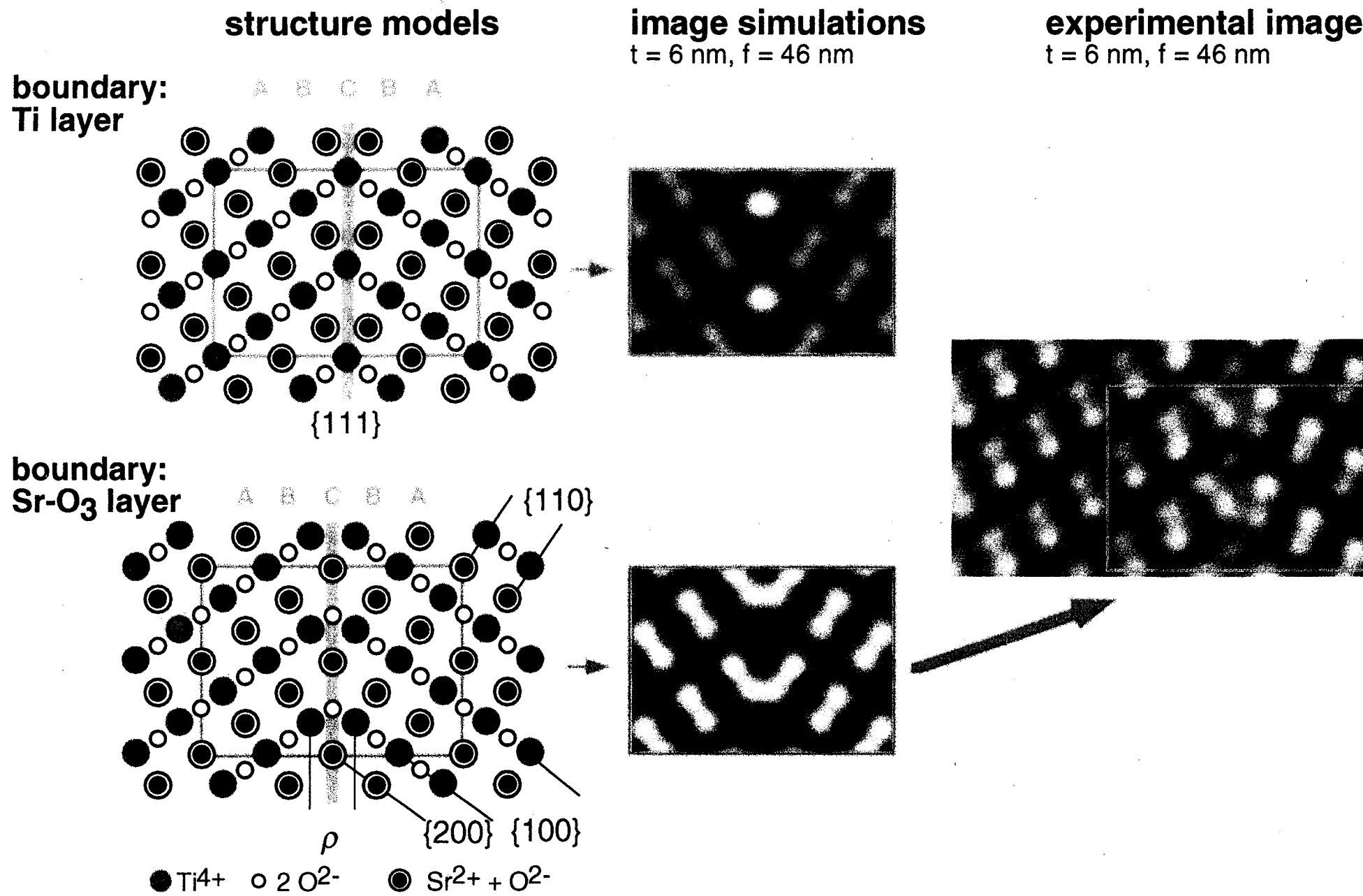


$\Sigma=3$, (111) grain boundary in <110> projection



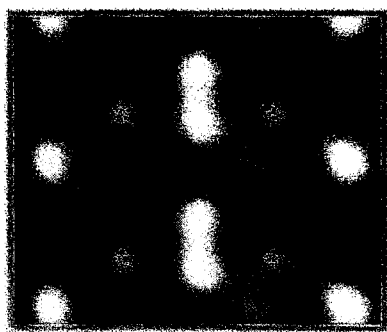
Kienzle

$\text{SrTiO}_3 \Sigma 3 (111)$ preliminary models



QHRTEM structure retrieval

HRTEM image



structure model



Structure retrieval

Determine imaging conditions

sample thickness t , defocus f
sample tilt, beam tilt

Construct

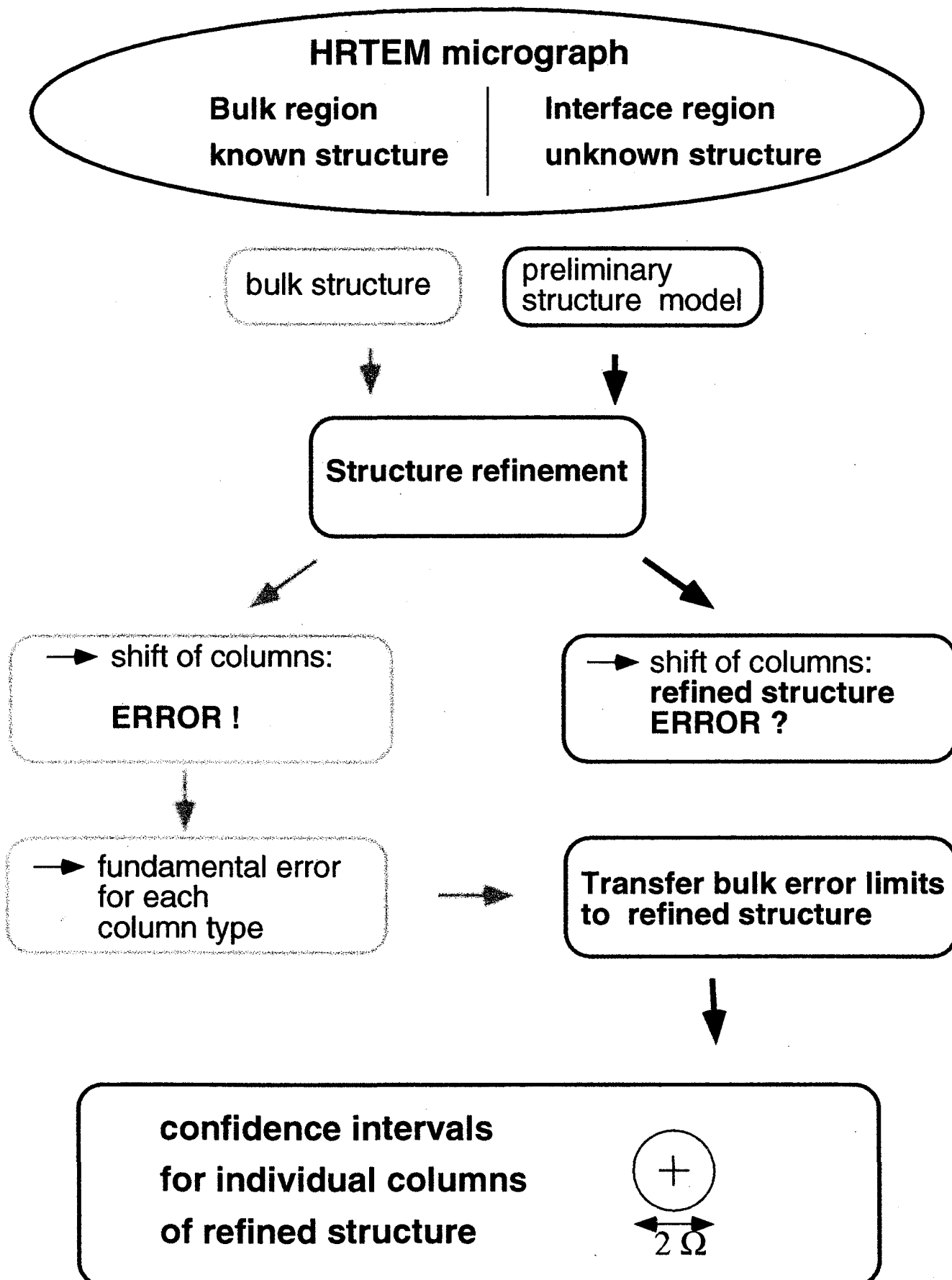
preliminary structure model

Structure refinement

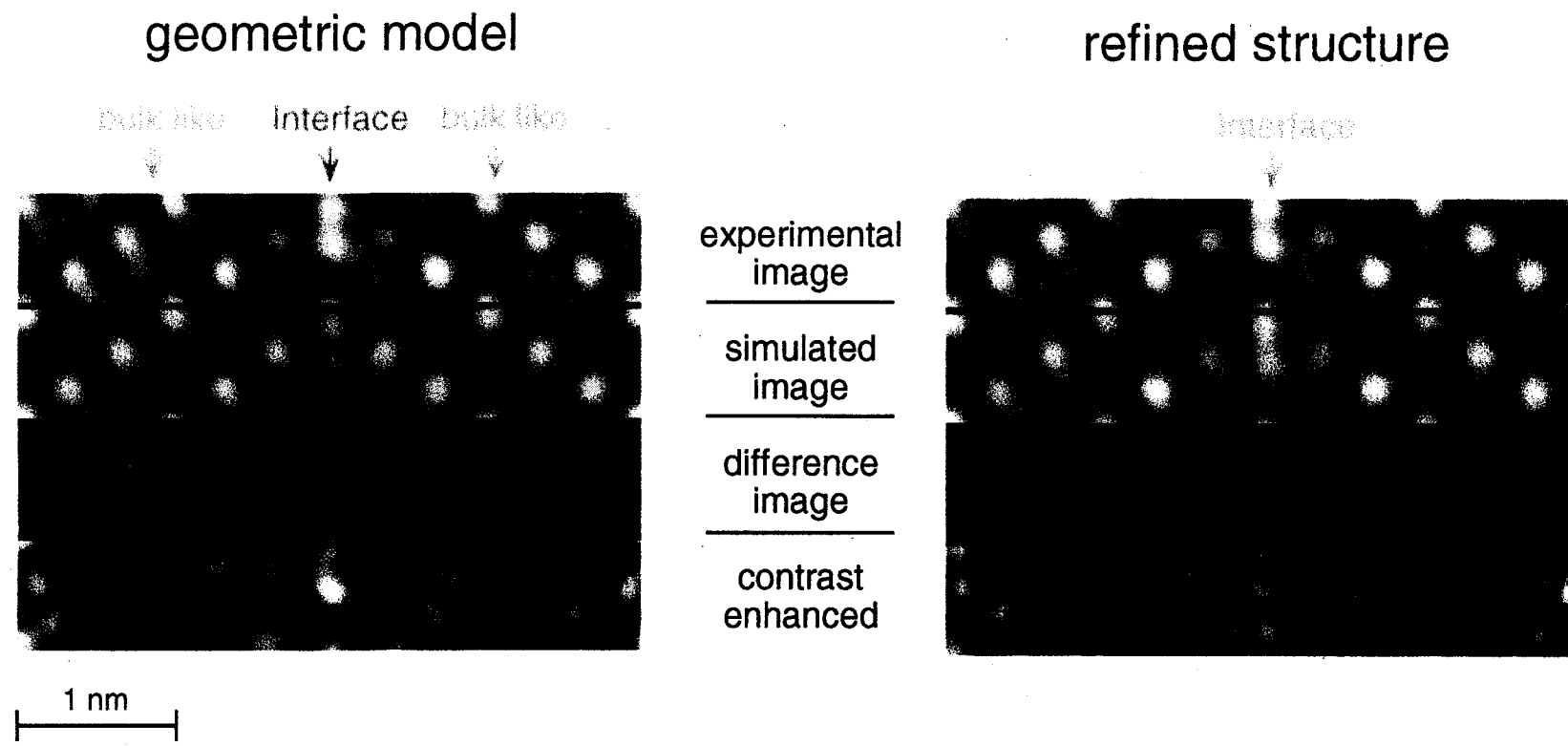
Iterative Digital image matching

$$D(\text{Sim}, \text{Exp}) = \min$$

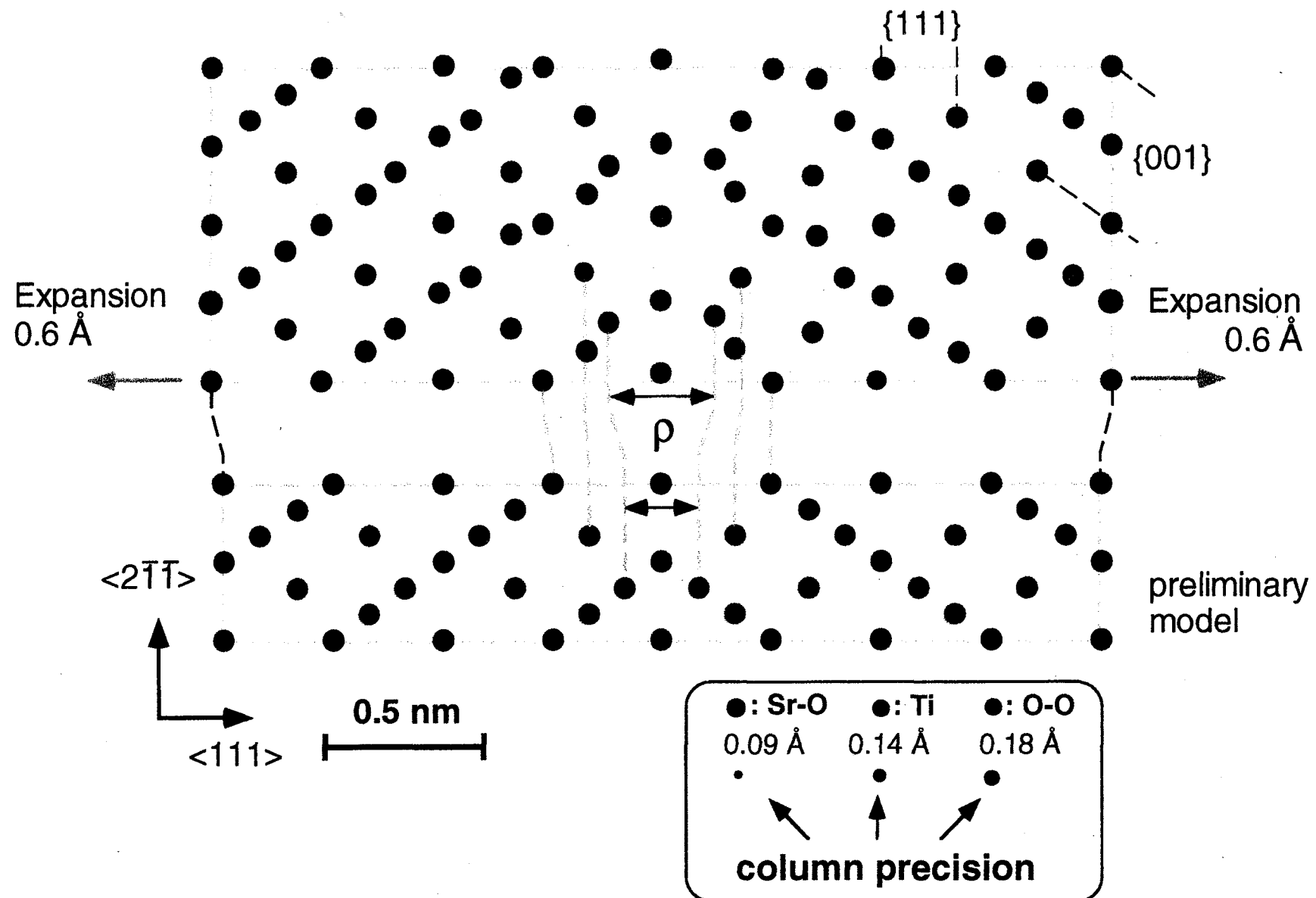
Quantification of error limits



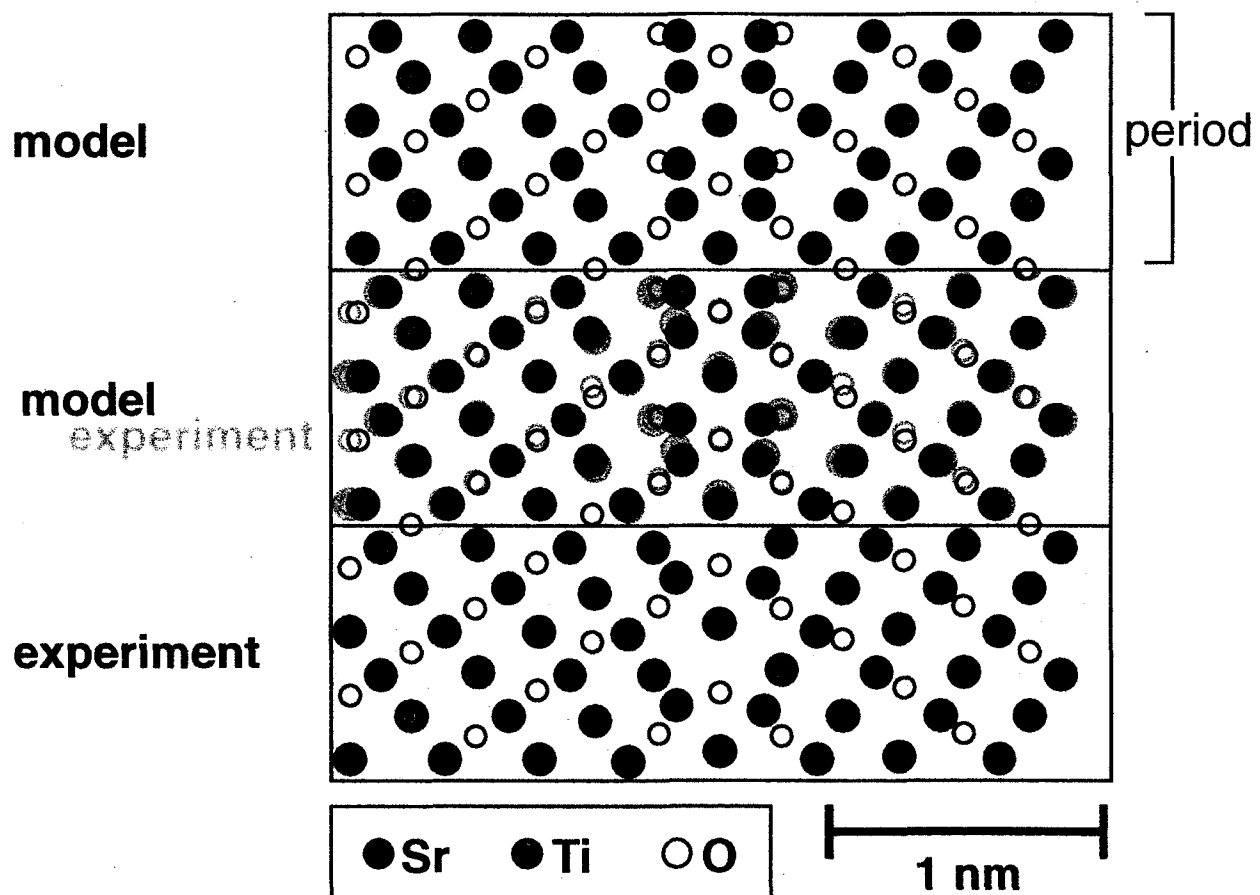
Iterative Digital Image Matching



Refined structure model



computer modelling versus experiment

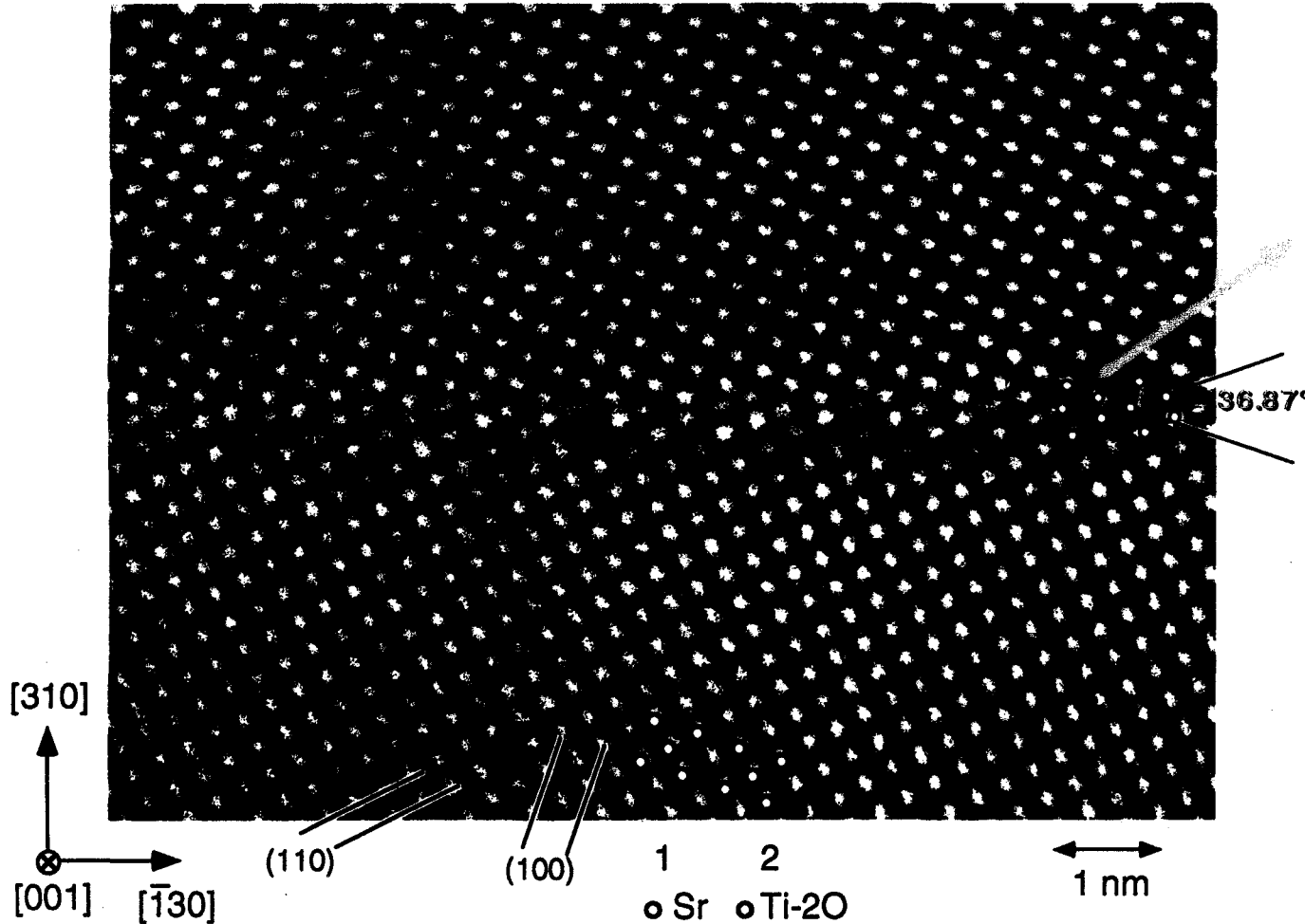


comparision	experiment	modelling
termination	Sr-O	Sr-O
coordination	Ti-O octahedra	Ti-O octahedra
excess volume:	expansion: + 0.6 Å	expansion + 0.3 Å
relaxation at gb	Sr-O inward vs Ti low	Sr-O inward vs Ti large

Near $\Sigma 5$ (310) grain boundary / structure

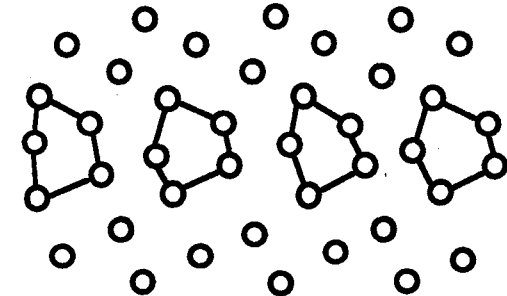
Doping level: Fe/Ti = 0.01 at.%

HRTEM JEM 4000EX

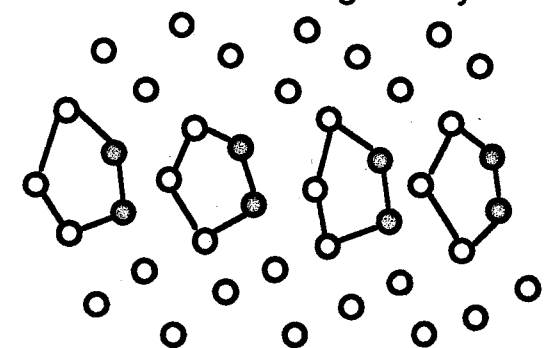


Structure models

Phasecontrast, preliminary



Z-contrast Browning/Pennycook

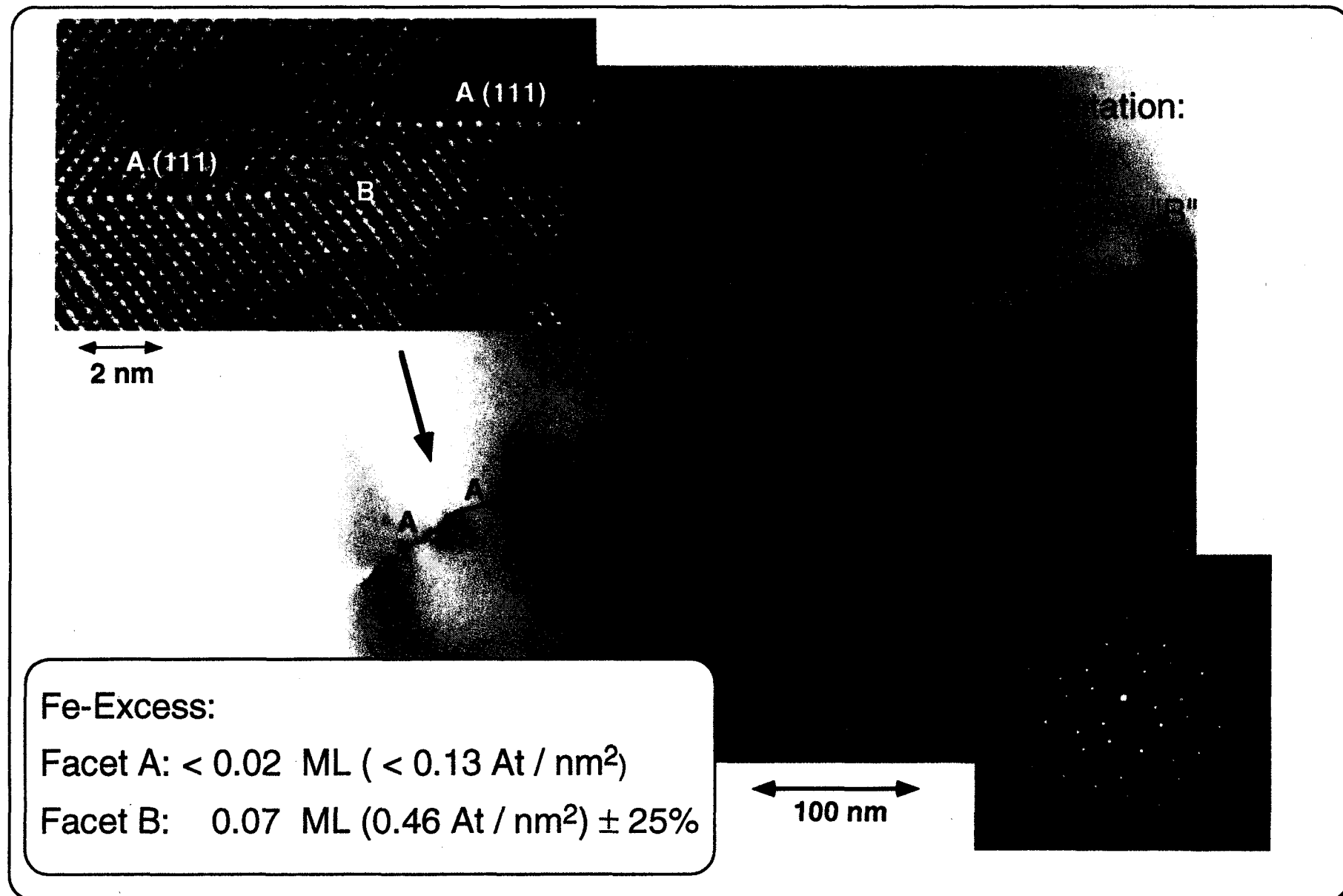


○ Sr complete
● half occupied

○ Ti complete
● half occupied

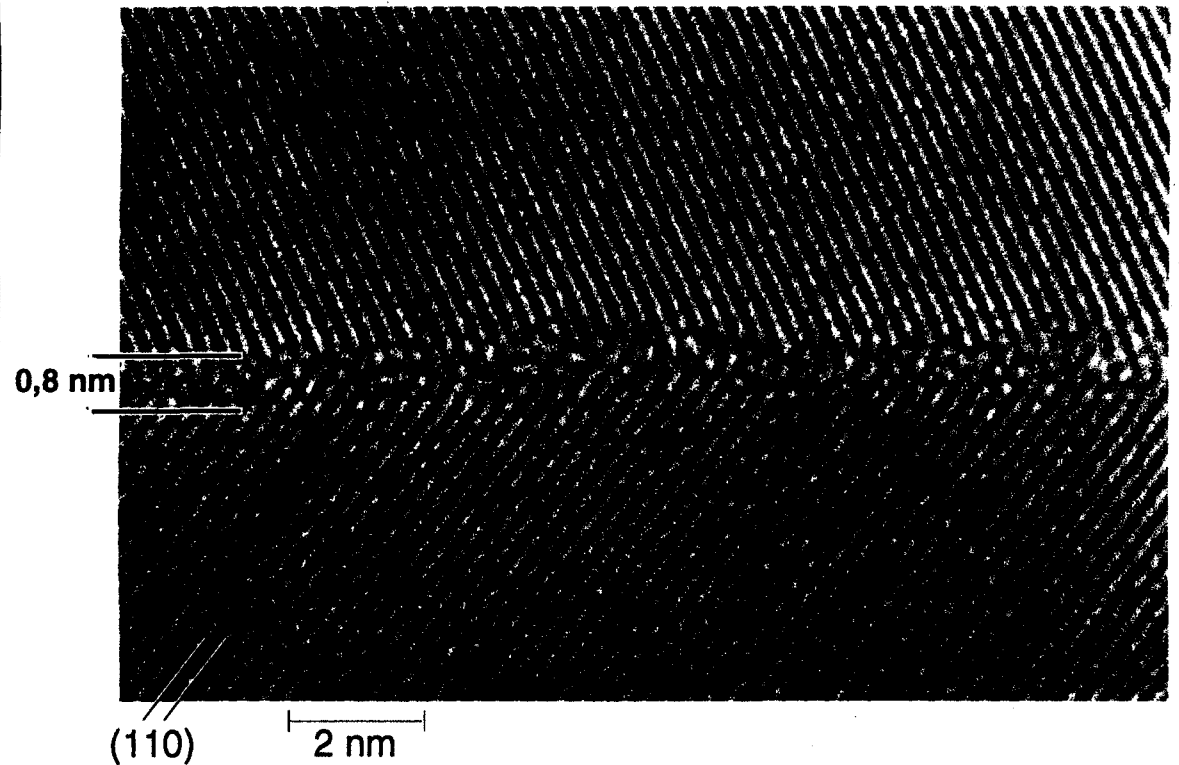
Near $\Sigma 3$ (111) grain boundary in polycrystalline SrTiO_3

Doping level: Fe / Ti = 0.4 at.%

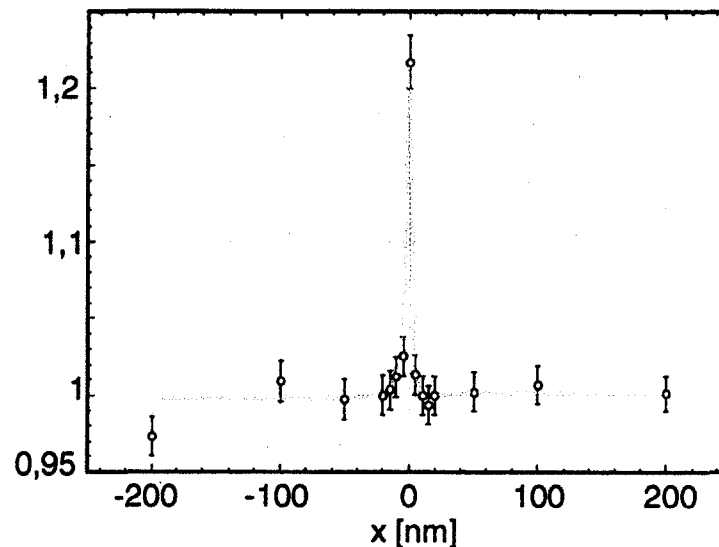
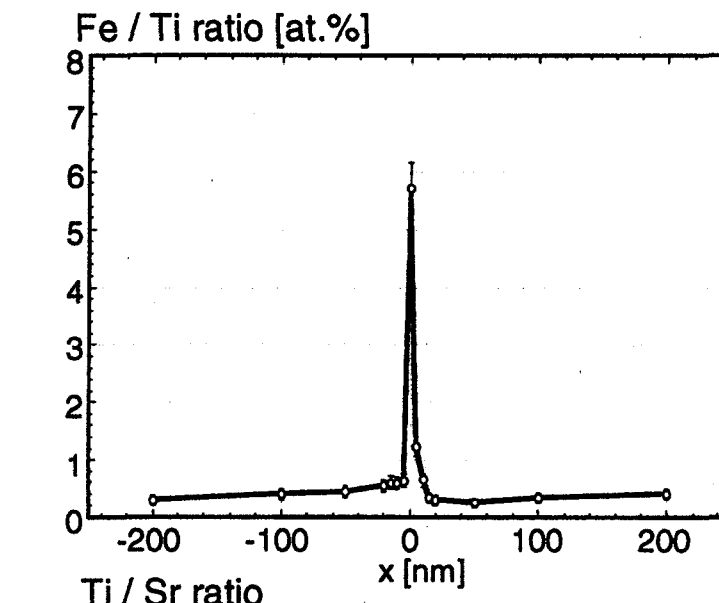


"general" grain boundaries in polycrystalline SrTiO₃

Doping level: Fe / Ti = 0.4 at.%



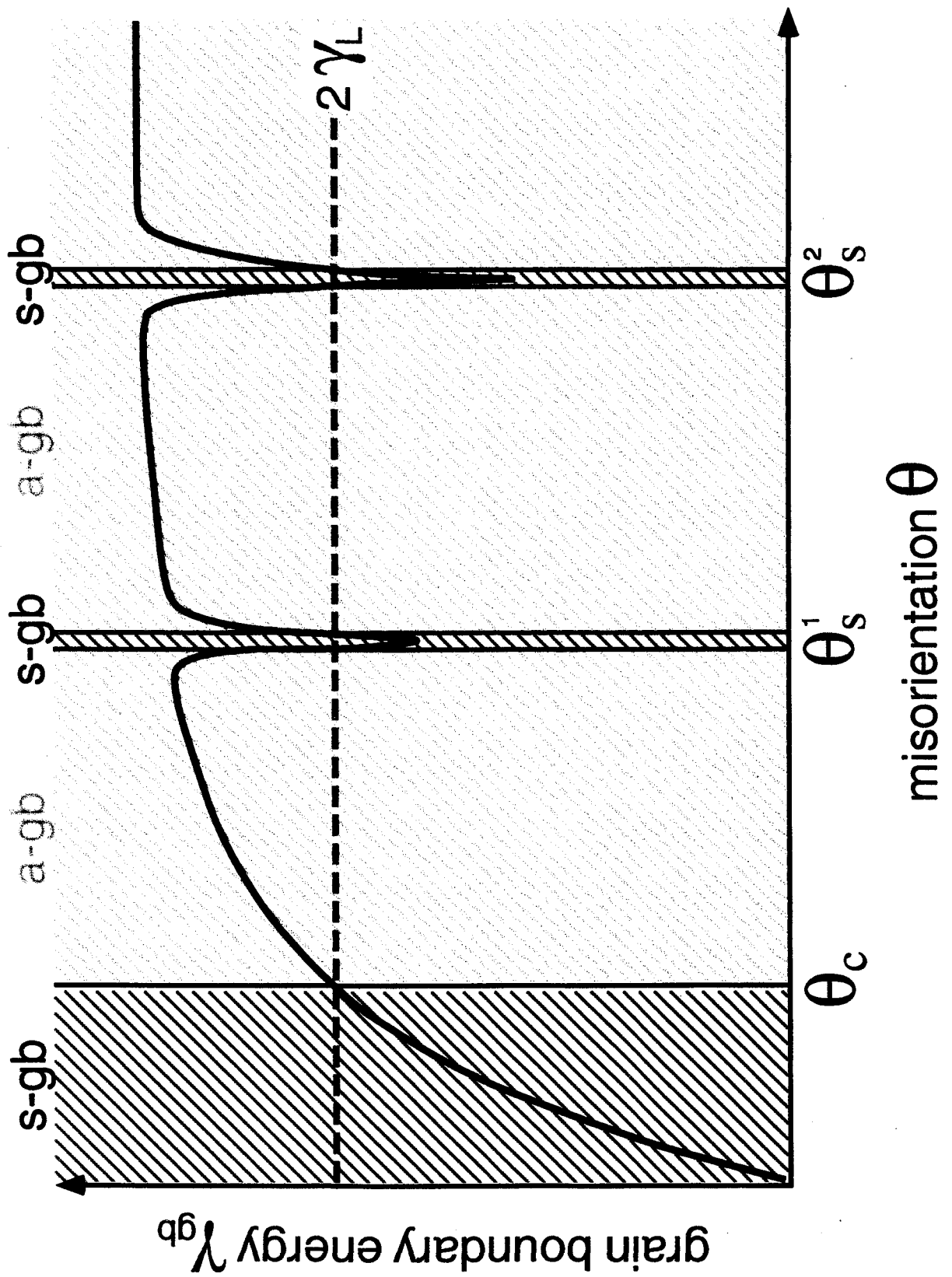
Profiles



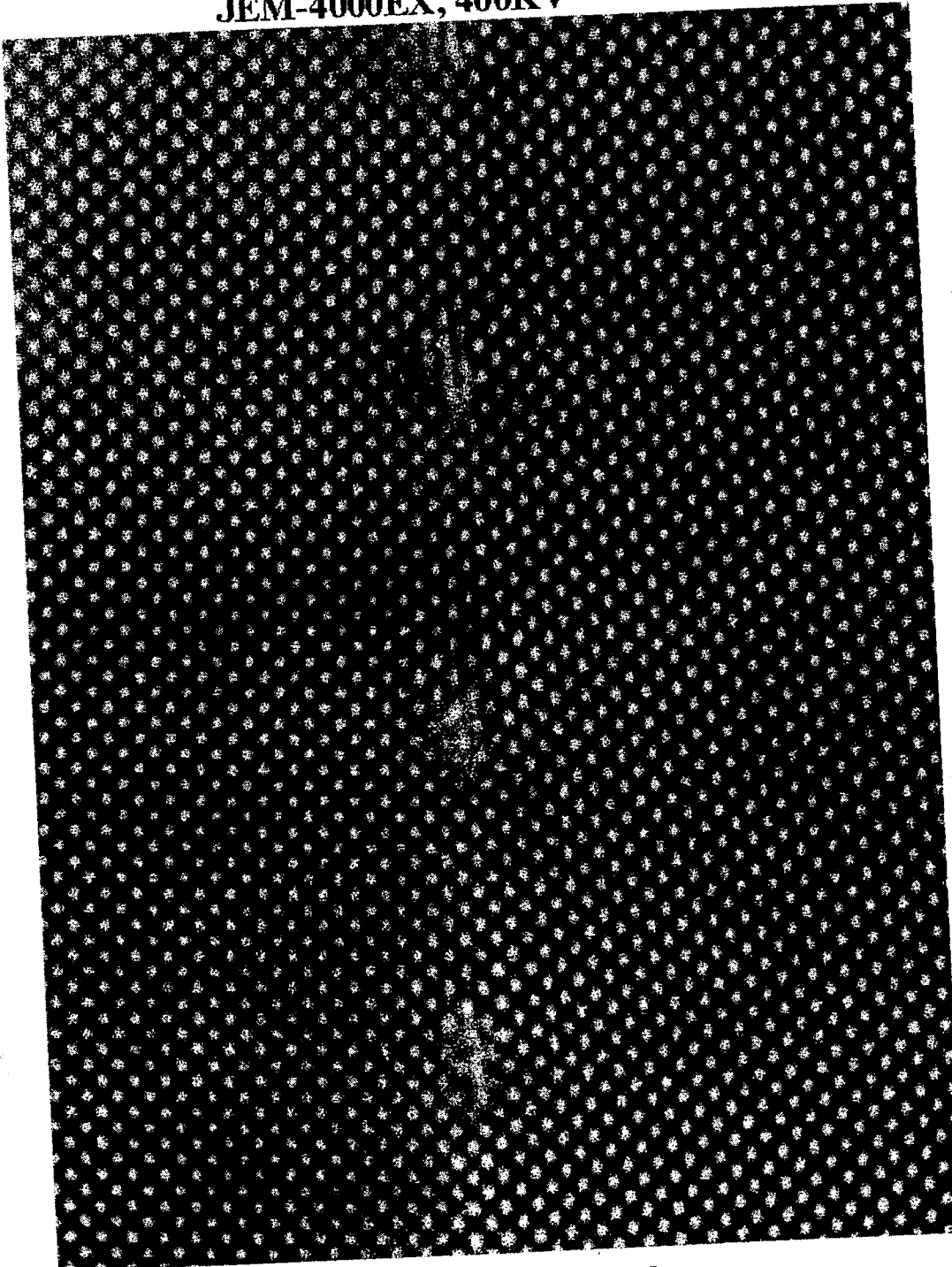
EDS

Fe-Excess: (0.61 ± 0.04) ML $(4.0 \text{ At} / \text{nm}^2)$

Ti-Excess: (1.3 ± 0.14) ML $(10.5 \text{ At} / \text{nm}^2)$



JEM-4000EX, 400KV



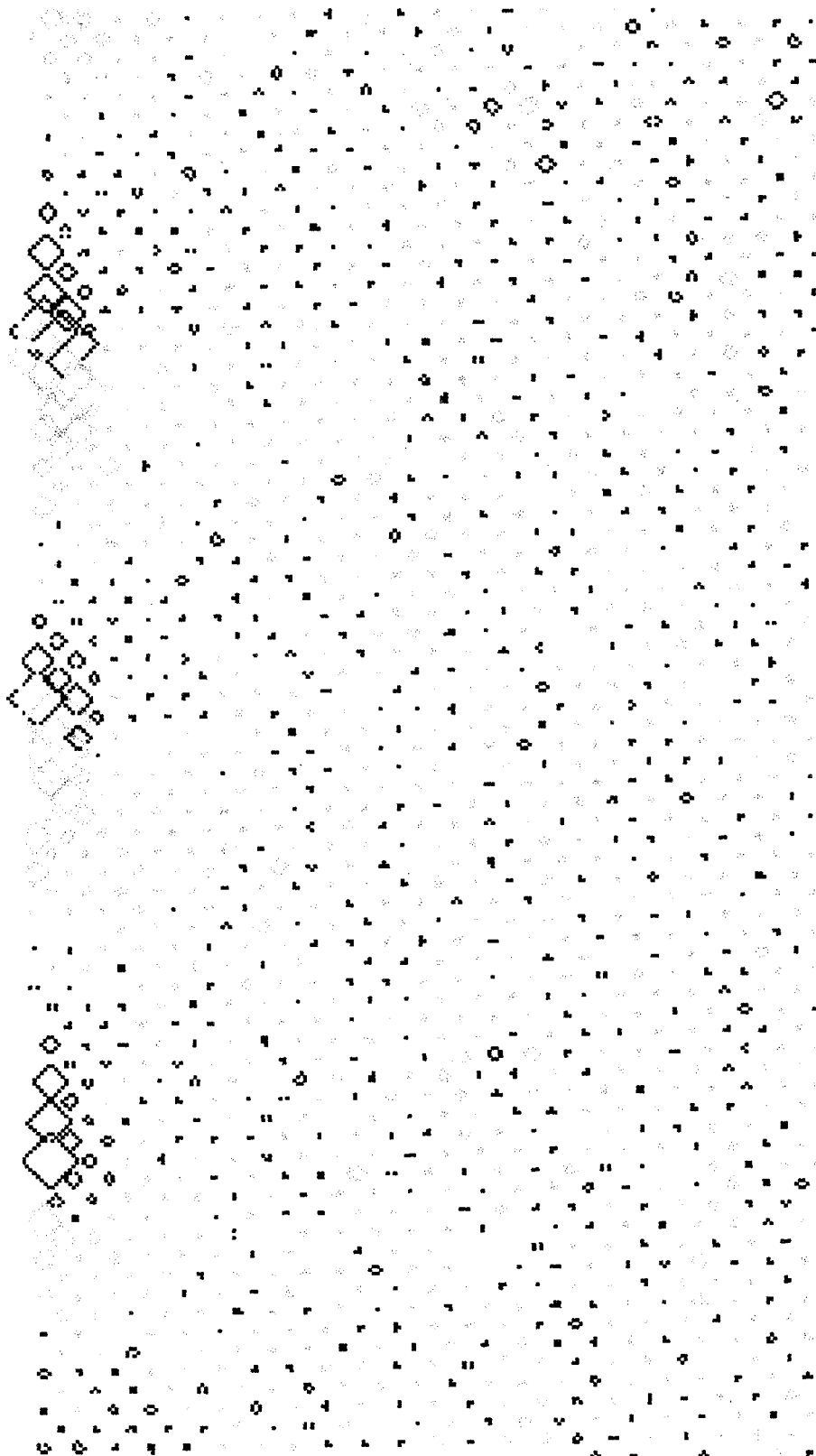
Courtesy of Oliver Kienzle

Small-angle grain boundary in SrTiO₃

1

1

1



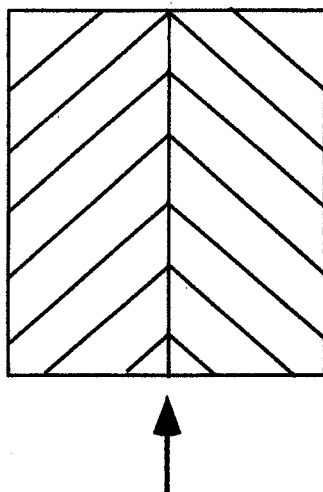
— Compression
Expansion

2 nm

Summary, conclusion and outlook

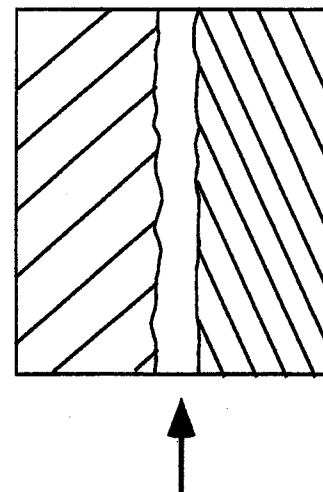
grain boundary structure \longleftrightarrow space charge region

a) special boundaries



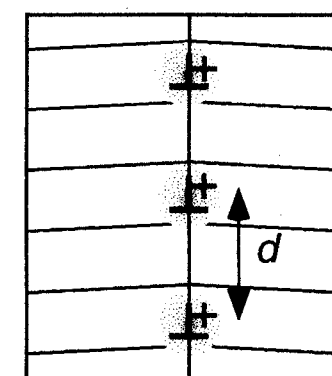
No detectable segregation
 $\Sigma=3$, (111) poly / bicrystal
 $\Sigma=5$, (310) bicrystal
HRTEM: "perfect structures"

b) amorphous film



Sr-deficient
Ti, Fe segregation
 $Ti_{0.75}Fe_{0.25}O_x$
HRTEM, ELNES:
amorphous GB core

c) low angle boundary



outlook

varying d
by misorientation
-> diffusion bonding

Correlation to diffusion across GB, electr. properties

S. Hutt(1999)
O. Kienzle
(J. Maier)

Motivation

Sc	Ti	V	Cr	Mn	Fe	Co	Ni	Cu	Zn
Y	Zr	Nb	Mo	Ti	Ru	Rh	Pd	Ag	Ge
La	Al	Cr	W	Fe	Os	Pt	Ir	Ag	Ge

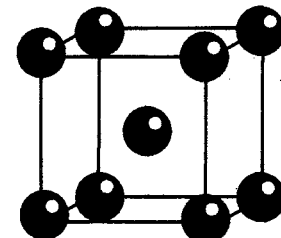
Lattice mismatch:

Mo > Ni > Cr > Pd

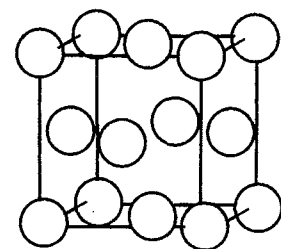
Reactivity:

Cr > Mo > Ni > Pd

bcc: Cr, Mo



fcc: Ni, Pd



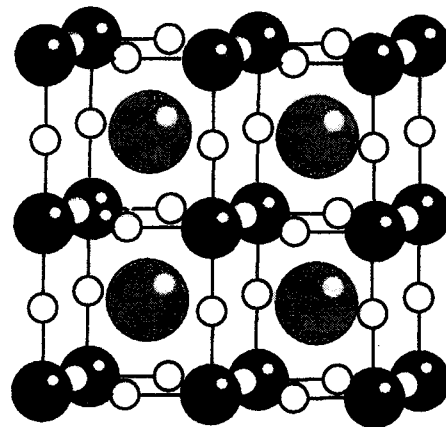
● Ti
○ O
● Sr

SrTiO_3

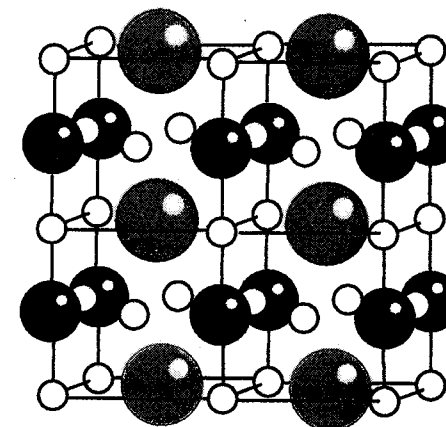
Surface Termination

TiO₂ terminated

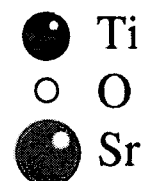
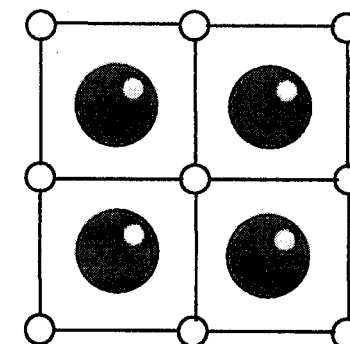
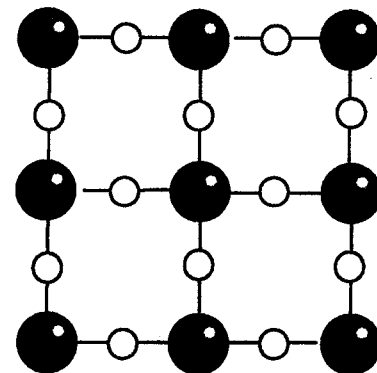
side view



SrO terminated



top view



Theory (T. Ochs, T. Classen, C. Elsässer):
metal on top of oxygen is energetically favoured!

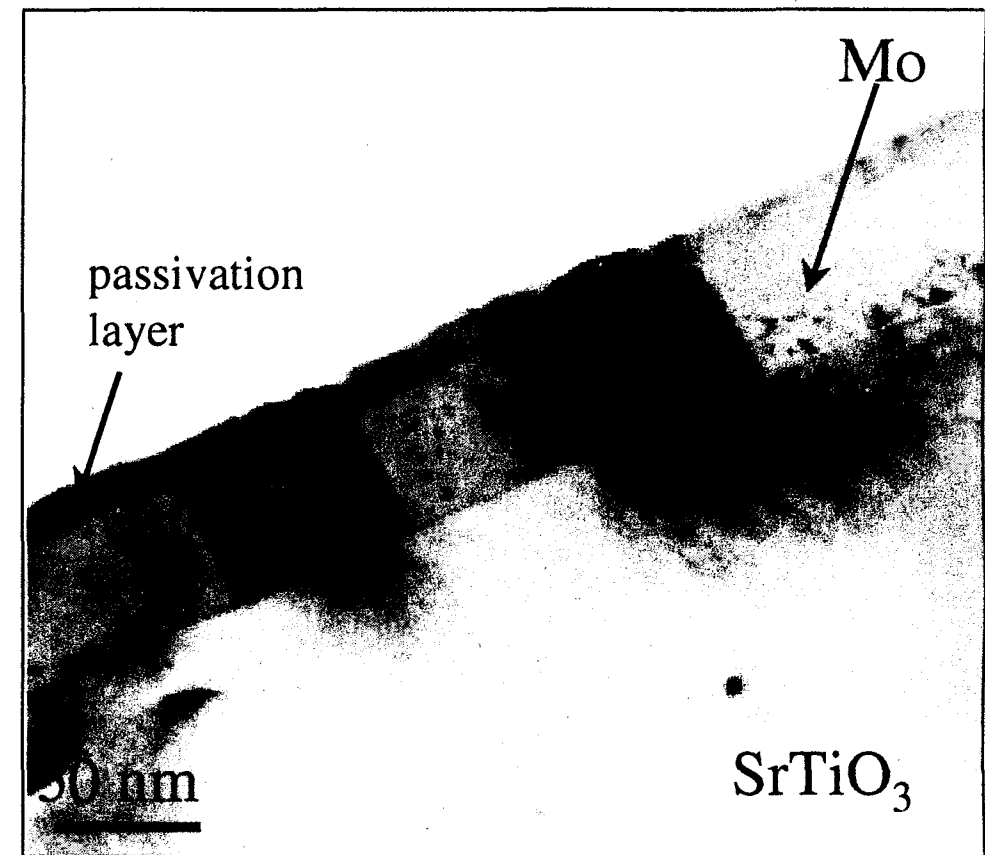
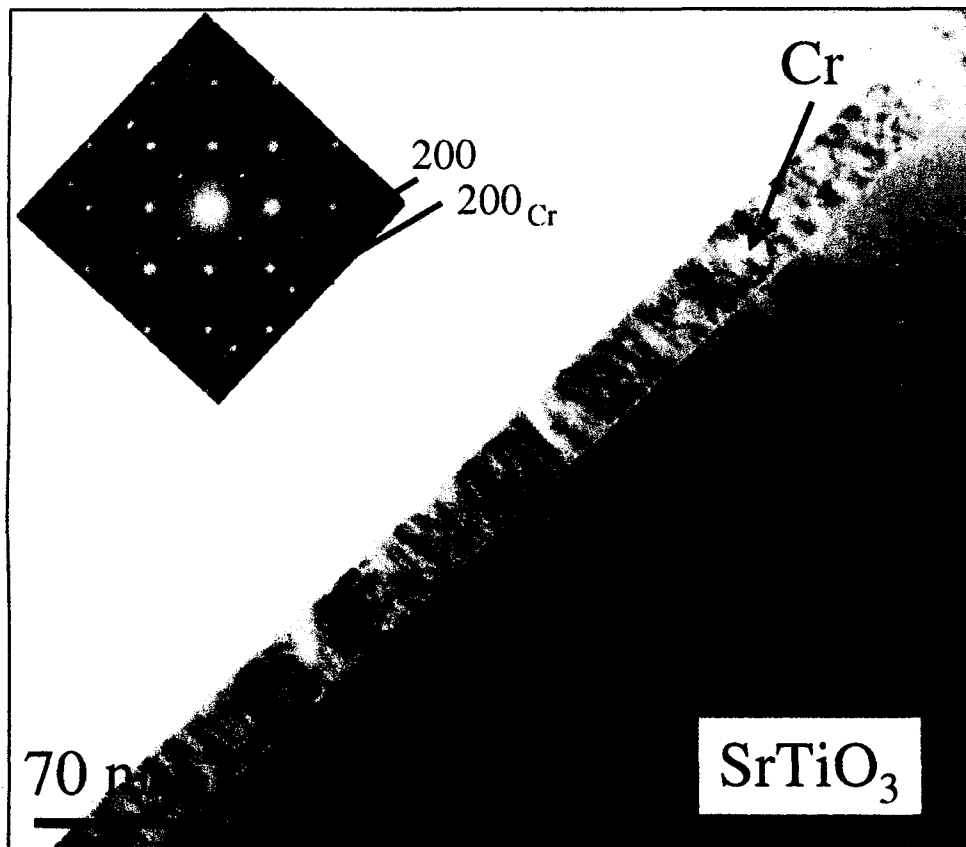
Experimental Details

Specimen fabrication

- nominal 35 - 100 nm thick metal films were grown on (001) SrTiO₃ by MBE in UHV (10^{-8} Pa)
- substrate temperature was varied between 65°C and 650°C for the various metals to obtain epitaxial films

Characterization

- conventional TEM: JEOL 2000FX (200 kV)
- high-resolution TEM: JEOL ARM1250 (1250 kV)
- analytical TEM: VG STEM HB 501 UX (100 kV)

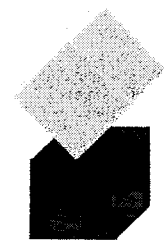


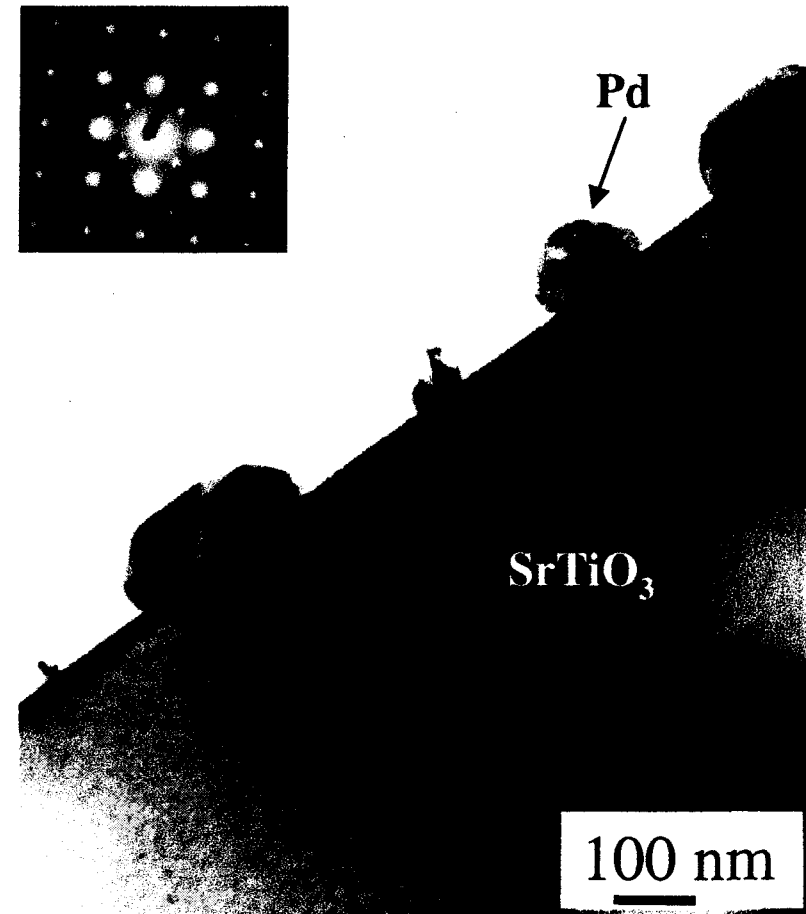
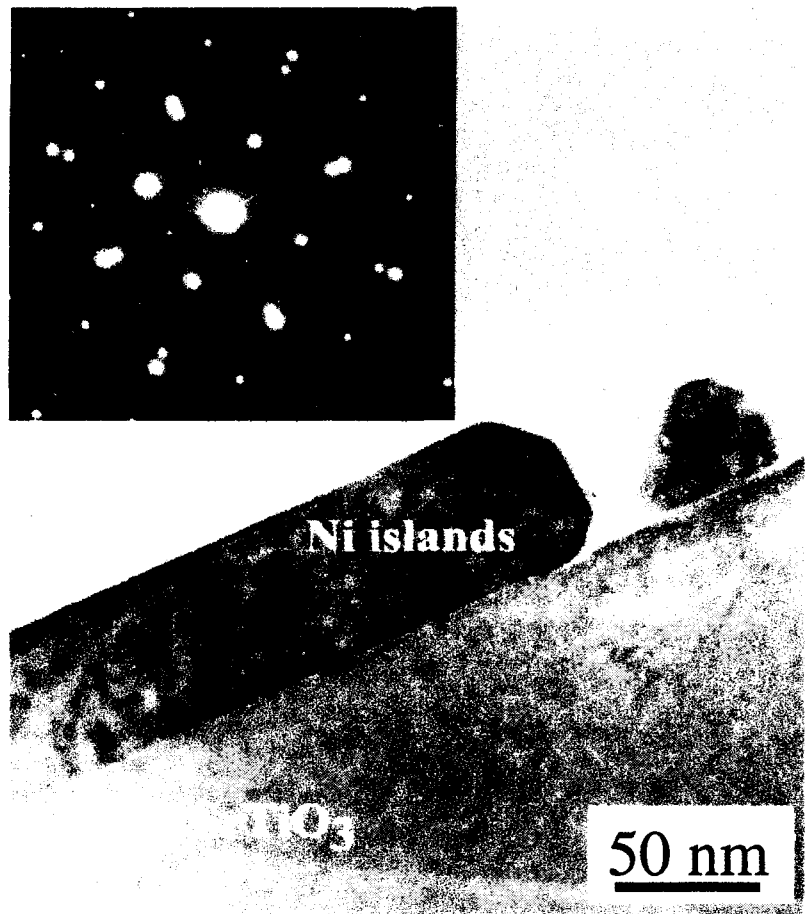
Orientation relationships



$$\begin{aligned} \{100\}_{\text{Cr}} &\parallel \{100\}_{\text{SrTiO}_3} \\ <110>_{\text{Cr}} &\parallel <100>_{\text{SrTiO}_3} \end{aligned}$$

$$\begin{aligned} \{110\}_{\text{Mo}} &\parallel \{100\}_{\text{SrTiO}_3} \\ \pm <100>_{\text{Mo}} &\parallel <100>_{\text{SrTiO}_3} \end{aligned}$$



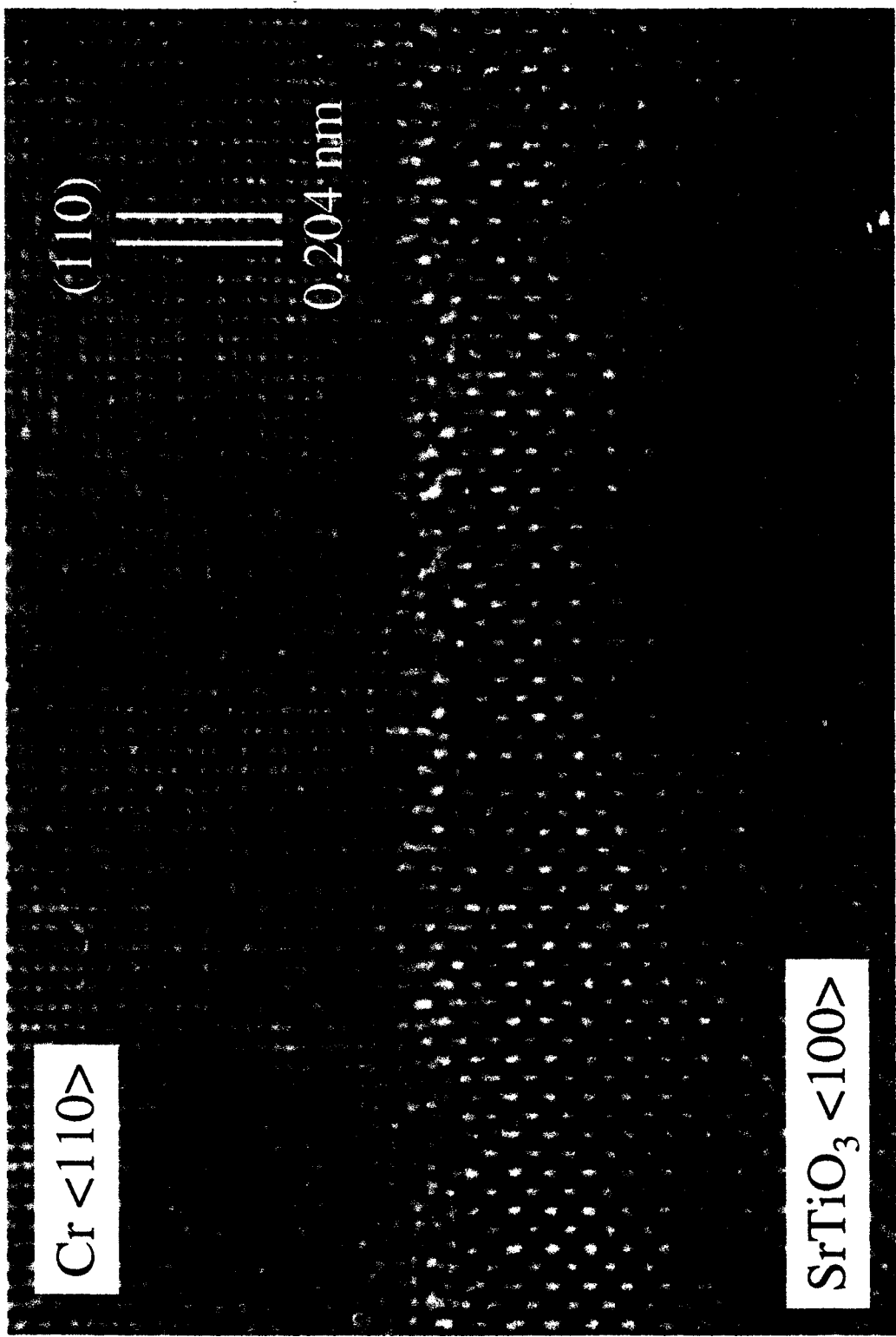


Orientation relationship

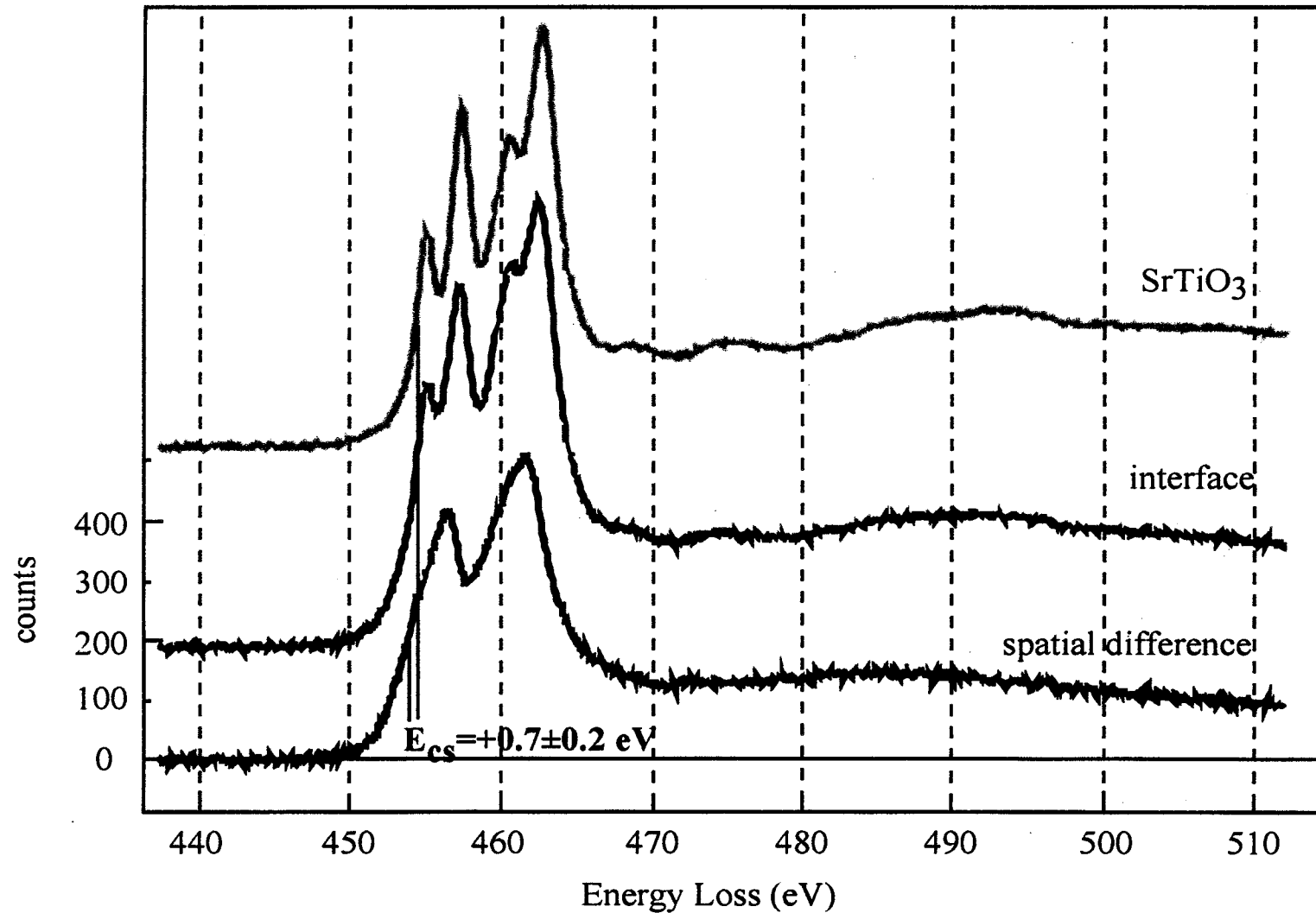
$$\begin{aligned}\{100\}_{\text{Metal}} &\parallel \{100\}_{\text{SrTiO}_3} \\ <100>_{\text{Metal}} &\parallel <100>_{\text{SrTiO}_3}\end{aligned}$$



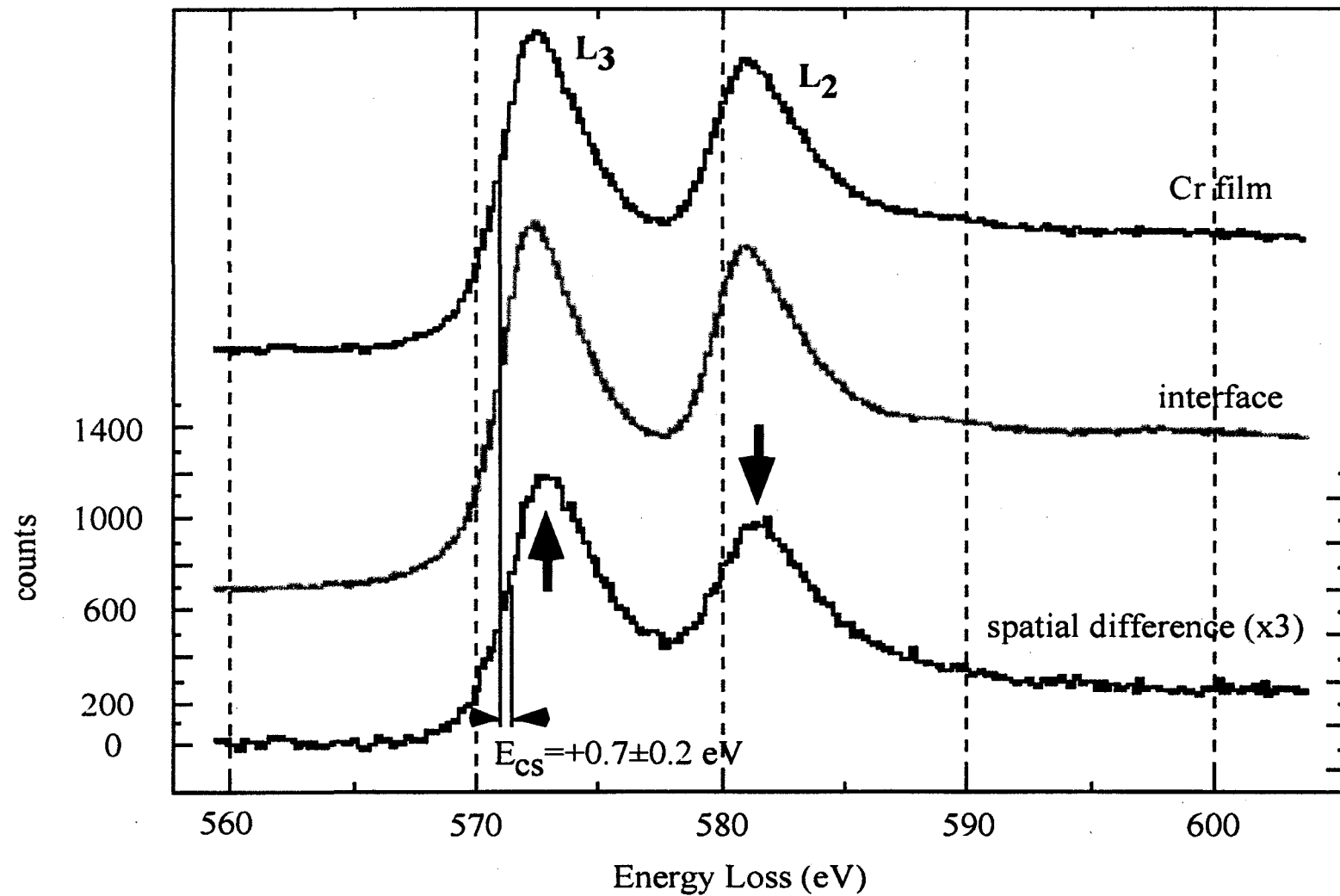
Metal
SrTiO₃



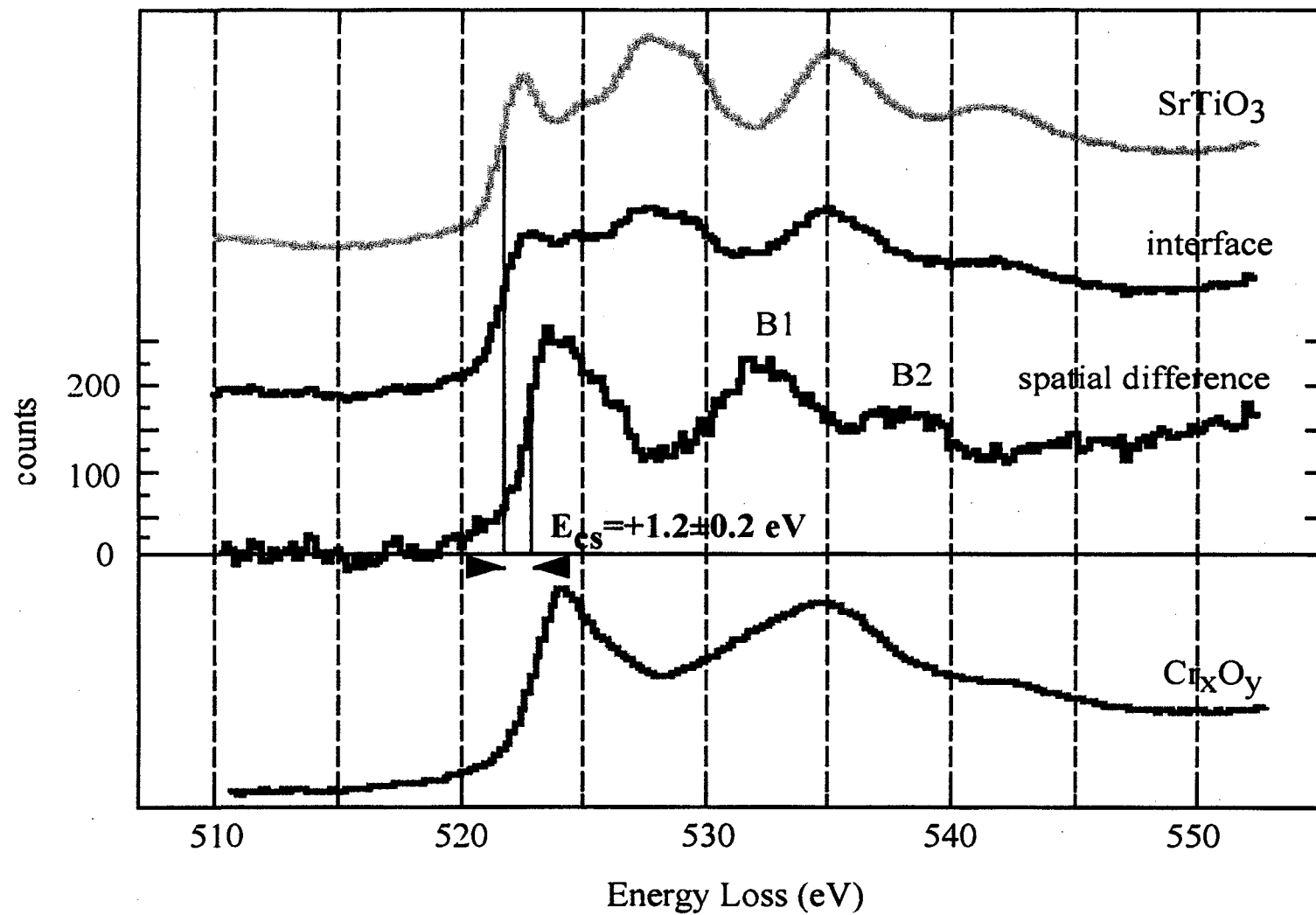
Ti L_{2,3} edge of Cr/SrTiO₃



Cr L_{2,3} edge of Cr/SrTiO₃



O K edge of Cr/SrTiO₃



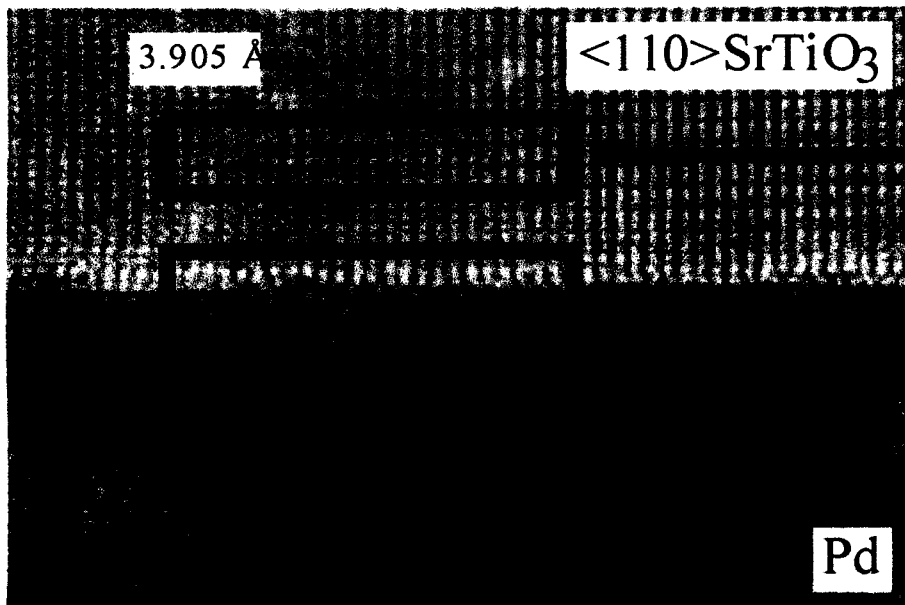
Analysis of the interfacial ELNES of Cr/SrTiO₃

- reduction of Ti at the interface
- reduced crystal field splitting
- O 2p - Cr 3d hybridization
- electron transfer from Cr to O

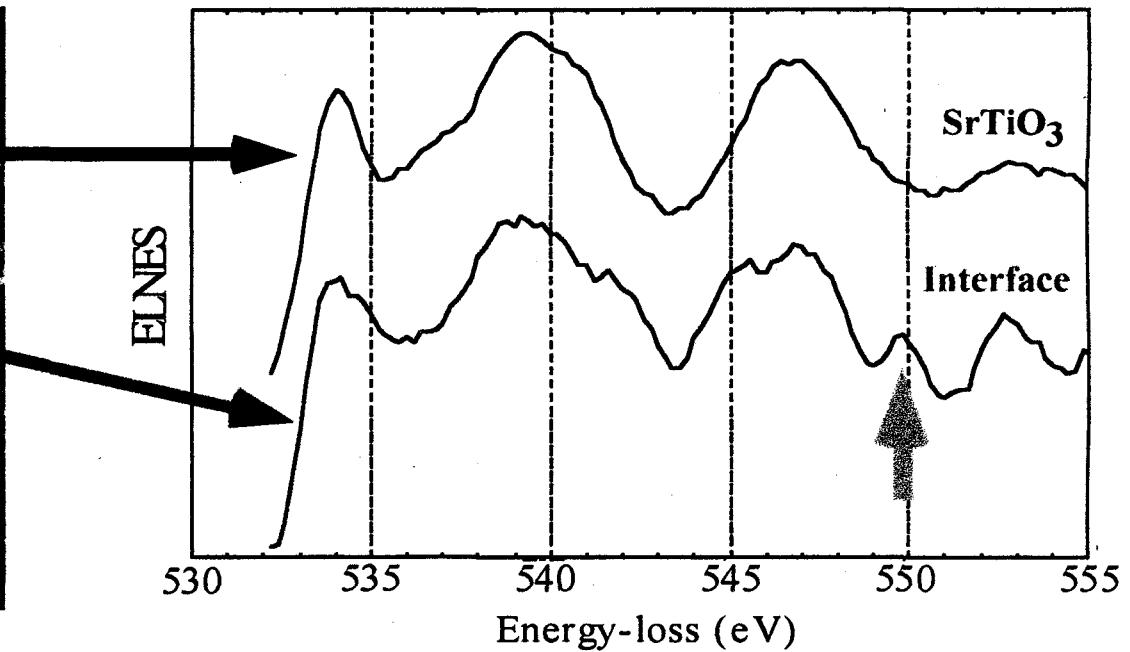
➡ mixed ionic-covalent bonding between Cr and SrTiO₃

O-K edge of Pd/SrTiO₃

Atomistic structure

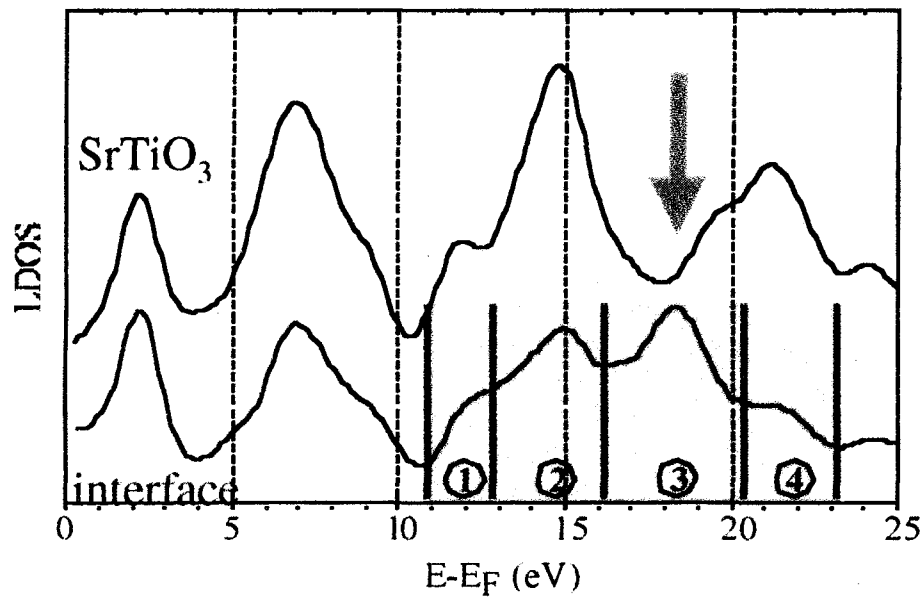


Electronic structure

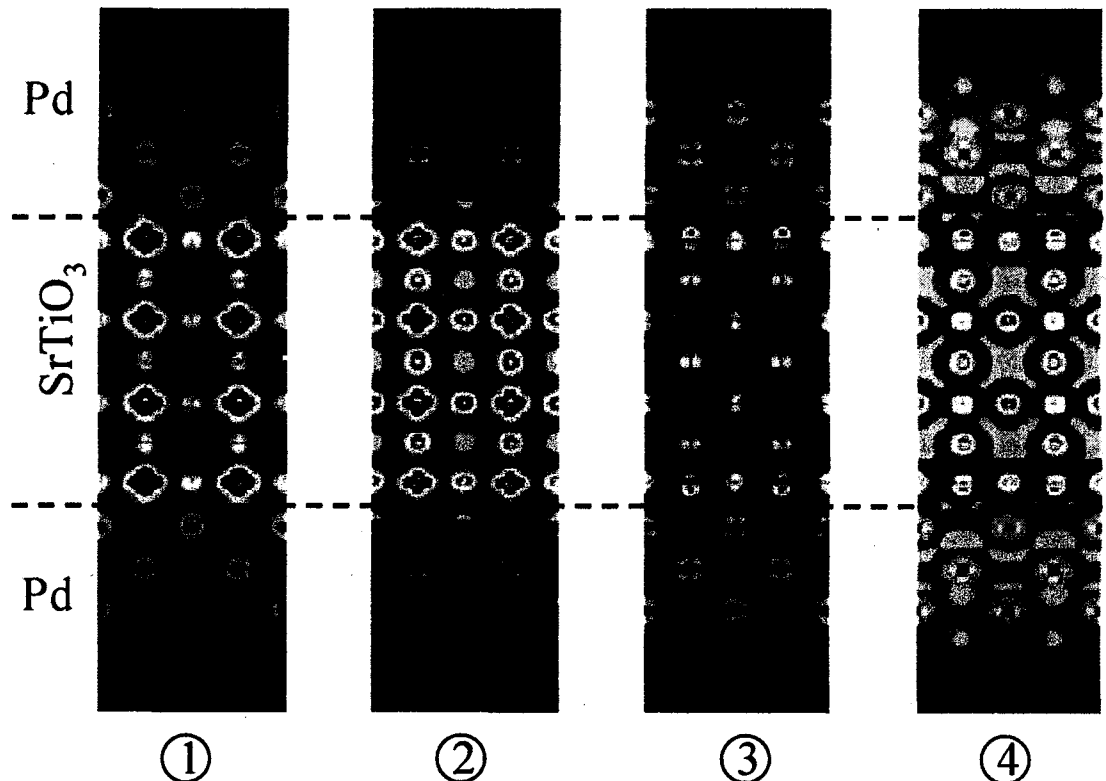


ab-initio calculations of Pd/SrTiO₃

Electronic structure



$|\Psi|^2$ distribution maps



- Oxygen p-PDOS
- additional peak in region 3
- similar line-shapes in comparison to the experimental data

- cut through Ti-O plane (i.e. 010,001-plane)
- appearance of interface specific components in region 3

K. van Benthem and C. Elsässer, unpublished

Analysis of the interfacial ELNES of Pd/SrTiO₃

- experiment and theory provide the same interfacial ELNES



- interaction between Pd and O
- Pd sits above the O of the TiO₂ terminated (001) SrTiO₃
- O 2p - Pd 4d hybridization

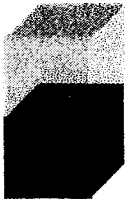


covalent bonding between Pd and SrTiO₃

Summary

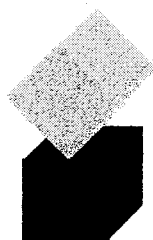
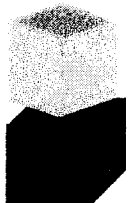
Pd/SrTiO₃ and Ni/SrTiO₃:

- epitaxial growth with cube-on-cube orientation relationship
- island growth
- the electronic structure of **Pd/SrTiO₃** is determined by experiment and theory



Cr/SrTiO₃ and Mo/SrTiO₃:

- epitaxial growth with cube-on-cube but 45° in-plane rotated for **Cr/SrTiO₃** and 45° out-plane rotated for **Mo/SrTiO₃**
- continuous film layers
- the electronic structure of **Cr/SrTiO₃** is determined by experiment



The Future of Microscopy

